



UNIVERSITI
MALAYSIA
KELANTAN

FYP FBKT

Preliminary Study of Utilizing Walnut Shell Waste for Clay-based Porous Ceramic Production

Mohamad AmirulAmin Bin Yusri
J20A0473

**A thesis submitted in fulfilment of the requirements for the
degree of Bachelor of Applied Science (Materials Technology)
with Honours**

**FACULTY OF BIOENGINEERING AND TECHNOLOGY
UMK**

2023

DECLARATION

I declare that this thesis entitled “Preliminary Study of Utilizing Walnut Shell Waste for Clay-based Porous Ceramic Production” is the results of my own research except as cited in the references.



Signature : amin

Student's Name : MOHAMAD AMIRULAMIN BIN YUSRI

Date : 8 January 2024

Verified by : _____

Signature


 **TS. DR. TEO PAO TER**
B. Eng, PhD (USM)
PENSYARAH KANAN
Fakulti Biokejuruteraan dan Teknologi
UNIVERSITI
MALAYSIA
KELANTAN

Supervisor's Name : TS. DR. TEO PAO TER

Stamp : _____

Date : 8 January 2024

ACKNOWLEDGEMENT

I would like to begin by expressing my endless gratitude to my creator, Allah SWT, for the direction and blessings that He gave upon me. It is because of His guidance and blessings that I have been able to successfully complete my Final Year Project (FYP), despite the difficulties that have been placed upon me. My heartfelt gratitude goes out to Him for providing me with the chance, the quality, and the health to finish this final year project.

I would like to use this opportunity to share my profound and heartfelt thanks to my research supervisor, Ts. Dr. Teo Pao Ter, from the Universiti Malaysia Kelantan. He has not only provided me with the chance to do research but also with essential assistance during the whole of this project. His vision, genuineness, and ambition have been a huge inspiration for me. Having the opportunity to work and learn under his direction was a tremendous honor and pleasure. I cannot express how appreciative I am for all he has provided for me. Aside from that, I would want to express my gratitude to him for his friendship, sensitivity, and wonderful sense of humor.

Throughout the course of my study, I would like to express my gratitude to the whole faculty and staff of the Faculty of Bioengineering and Technology at the University of Malaysia Kelantan for their helpful assistance and cooperative efforts.

Last but not least, I would want to express my gratitude to all of my closest friends who have never stopped providing me with support, knowledge, and help in order to finish this project. Many thanks for everything, and I wish you the very best of success. In addition, I would want to express my gratitude to those individuals who have indirectly contributed remarks and assistance.

Preliminary Study of Utilizing Walnut Shell Waste for Clay-based Porous Ceramic Production

ABSTRACT

Ceramics that have a substantial amount of porosity, ranging from 20% to 95%, are referred to as porous ceramics. In general, porous ceramics have a number of desirable properties, including high mechanical strength, resistance to abrasion, chemical and thermal stability, and other properties. Compared to other types of ceramic structures, porous network ceramic structures are comparatively lightweight, have a low density, a low mass, and poor heat conductivity. For the purpose of producing porous ceramic, pore-forming agents, also known as PFA, are added to the ceramic powder. In order to manufacture PFA, the powder compaction process was used. For the purpose of producing porous ceramic, researchers investigated the possibility that food waste, such as coffee grounds, peanut shells, and banana peels, might be used as a PFA. The high moisture content of food waste might make the process of preparation more difficult than it would otherwise be. This research aims to evaluate the suitability of walnut shell as a PFA for porous ceramics and to investigate the effect of wt.% walnut shell and sintering temperature on the physical and mechanical properties of porous ceramics. A procedure known as sacrificial fugitive was used in order to create porous ceramic. The water absorption test, apparent porosity, bulk density, linear shrinkage, and crystalline phase (XRD characterisation) were the methods that were used in order to determine the physical properties. Compressive strength was used in order to get better understanding of the mechanical properties. An increase in the weight % of walnut shell (WS) in the porous ceramic was shown to have a strongly impact on the compressive strength of the material while simultaneously increasing the porosity of the material. When the sintering temperature is 950°C, the porous ceramic that contains walnut shell has the best strength at 10 wt.% WS, and the lowest strength is 20 wt.% WS when the sintering temperature is 850°C. When the porous ceramic was combined with 10 wt.% WS and the sintering temperature was set at 950°C, the composition and sintering characteristics were found to be well-balanced.

Keywords: Walnut Shell (WS), Pore-Forming Agent (PFA), Porous Ceramic

Kajian Awal Penggunaan Sisa Tempurung Walnut untuk Pengeluaran Seramik Berliang Berasaskan Tanah Liat

Abstrak

Seramik yang mempunyai jumlah keliangan yang besar, antara 20% hingga 95%, dirujuk sebagai seramik berliang. Secara umum, seramik berliang mempunyai beberapa sifat yang diinginkan, termasuk kekuatan mekanikal yang tinggi, ketahanan terhadap lelasan, kestabilan kimia dan haba, dan sifat-sifat lain. Berbanding dengan jenis struktur seramik lain, struktur seramik rangkaian berliang adalah secara perbandingan ringan, mempunyai ketumpatan rendah, jisim rendah dan kekonduksian haba yang lemah. Untuk tujuan menghasilkan seramik berliang, agen pembentuk liang, juga dikenali sebagai PFA, ditambah kepada serbuk seramik. Untuk menghasilkan PFA, proses pemadatan serbuk telah digunakan. Untuk tujuan menghasilkan seramik berliang, penyelidik menyiasat kemungkinan sisa makanan, seperti serbuk kopi, kulit kacang dan kulit pisang, mungkin digunakan sebagai PFA. Kandungan lembapan sisa makanan yang tinggi mungkin menjadikan proses penyediaan lebih sukar daripada yang sepatutnya. Penyelidikan ini bertujuan untuk menilai kesesuaian kulit walnut sebagai PFA untuk seramik berliang dan untuk menyiasat kesan berat kulit walnut dan suhu pensinteran ke atas sifat fizikal dan mekanikal seramik berliang. Prosedur yang dikenali sebagai pelarian korban digunakan untuk menghasilkan seramik berliang. Ujian penyerapan air, keliangan ketara, ketumpatan pukal, pengecutan linear, dan fasa kristal (pencirian XRD) adalah kaedah yang digunakan untuk menentukan sifat fizikal. Kekuatan mampatan digunakan untuk mendapatkan pemahaman yang lebih baik tentang sifat mekanikal. Peningkatan dalam % berat cengkerang walnut (WS) dalam seramik berliang ditunjukkan mempunyai kesan yang kuat ke atas kekuatan mampatan bahan dan pada masa yang sama meningkatkan keliangan bahan. Apabila suhu pensinteran ialah 950°C, seramik berliang yang mengandungi cangkerang walnut mempunyai kekuatan terbaik pada 10 wt.% WS, dan kekuatan terendah ialah 20 wt.% WS apabila suhu pensinteran ialah 850°C. Apabila seramik berliang digabungkan dengan 10 wt.% WS dan suhu pensinteran ditetapkan pada 950°C, komposisi dan ciri pensinteran didapati seimbang.

Kata kunci: Kulit Walnut (WS), Agen Pembentuk Liang (PFA), Seramik Berliang

TABLE OF CONTENTS

CHAPTER 1	1
INTRODUCTION	1
1.1 Background of Study	1
1.2 Problem Statement.....	2
1.3 Expected Output	3
1.4 Objective.....	3
1.5 Scope of Study	4
1.6 Significances of Study	4
CHAPTER 2	5
LITERATURE REVIEW	5
2.1 Introduction to Porous Ceramic.....	5
2.1.1 Formulation of Porous Ceramic.....	6
2.1.2 Kaolin Clay	6
2.1.3 Pore-Forming Agent (PFA)	7
2.1.4 Summary	8
2.2 Inorganic PFA as Production of Porous Ceramic.....	9
2.2.1 Types of Inorganic PFA.....	9
2.3 Organic PFA as Production of Porous Ceramic	10
2.3.1 Types of Organic PFA	10
2.4 Physical and Mechanical Properties of Porous Ceramic	11

2.4.1	Inorganic PFA.....	12
2.4.2	Organic PFA	13
2.4.3	Summary.....	14
2.5	Walnut Shell	15
2.5.1	FTIR Analysis of Walnut Shell	16
2.6	Overall Summary.....	17
CHAPTER 3		18
MATERIALS AND METHODS.....		18
3.1	Research Flow	18
3.2	Materials	20
3.2.1	Walnut Shell	20
3.2.2	Kaolin Clay	20
3.3	Methods	20
3.3.1	Water Absorption Characterization	22
3.3.2	Linear Shrinkage.....	23
3.3.3	Compressive Strength	24
3.3.4	XRD Analysis	24
3.3.5	Fourier Transform Infrared Spectroscopy (FTIR).....	25
3.3.6	Differential Scanning Calorimetry.....	25
3.4	General Full Factorial Design (GFFD).....	25
CHAPTER 4		27
Result and Discussion		27

4.1 Characterization of Raw Material.	27
4.1.1 FTIR Analysis of Walnut Shell	27
4.1.2 XRD Analysis of Kaolin Clay	28
4.1.3 DSC Analysis of Ceramic Mixture.....	30
4.2 General Full Factorial Design	34
4.2.1 Experimental Design Matrix	35
4.2.2 Model Adequacy Checking	37
4.2.3 Analysis of Variance (ANNOVA)	41
4.2.4 Main Effects and Interaction Plots	45
4.2.5 Contour plot and its application	53
4.3 XRD Analysis Incorporated with Walnut Shell	56
CHAPTER 5	60
5.1 Conclusion.....	60
5.2 Recommendations	61
REFERENCES	62

LIST OF TABLES

Table 2.1: Comparison of the mechanical and physical properties of all of the inorganic PFA.....	12
Table 2.2: Comparison of the mechanical and physical properties of all of the organic PFA.....	13
Table 3.1: Experimental design matrix for general full factorial design (GFFD).....	26
Table 4.1: Experimental design matrix for general full factorial design (GFFD).....	35
Table 4.2 (a): ANOVA for linear shrinkage of porous ceramic added with WS.....	42
Table 4.2 (b): ANOVA for water absorption of porous ceramic added with WS.....	42
Table 4.2 (c): ANOVA for apparent porosity of porous ceramic added with WS.....	43
Table 4.2 (d): ANOVA for bulk density of porous ceramic added with WS.....	43
Table 4.2 (e): ANOVA for compressive strength of porous ceramic added with WS.....	43
Table 4.3: Mohs hardness scale of the crystalline phase.....	59

LIST OF FIGURES

Figure 2.1: FTIR peak of walnut shell (Uddin & Nasar, 2020).....	16
Figure 3.1: Research flow stage 1 for porous ceramic incorporated with WS.....	18
Figure 3.2: Research flow stage 2 for porous ceramic incorporated with WS.....	19
Figure 4.1: FTIR pattern of walnut shell powder.....	27
Figure 4.2: XRD analysis of raw kaolin clay.....	29
Figure 4.3 (a): DSC analysis for raw WS powder.....	30
Figure 4.3 (b): DSC analysis for powder mixture incorporated with 0wt.% WS.....	31
Figure 4.3 (c): DSC analysis for powder mixture incorporated with 10wt.% WS.....	32
Figure 4.3 (d): DSC analysis for powder mixture incorporated with 20wt.% WS.....	33
Figure 4.4 (a): Residual plots for linear shrinkage; (i) Normal probability plot, (ii) Histogram of frequency versus residual, (iii) Residual versus fits, (iv) Residual versus observation order of data.....	38
Figure 4.4 (b): Residual plots for water absorption; (i) Normal probability plot, (ii) Histogram of frequency versus residual, (iii) Residual versus fits, (iv) Residual versus observation order of data.....	38
Figure 4.4 (c): Residual plots for apparent porosity; (i) Normal probability plot, (ii) Histogram of frequency versus residual, (iii) Residual versus fits, (iv) Residual versus observation order of data.....	39
Figure 4.4 (d): Residual plots for bulk density; (i) Normal probability plot, (ii) Histogram of frequency versus residual, (iii) Residual versus fits, (iv) Residual versus observation order of data.....	39
Figure 4.4 (e): Residual plots for compressive strength; (i) Normal probability plot, (ii) Histogram of frequency versus residual, (iii) Residual versus fits, (iv) Residual versus observation order of data.....	40
Figure 4.5 (a): Main effects plots for linear shrinkage.....	45
Figure 4.5 (b): Main effects plots for water absorption.....	46
Figure 4.5 (c): Main effects plots for apparent porosity.....	46
Figure 4.5 (d): Main effects plots for bulk density.....	47

Figure 4.5 (e): Main effects plots for compressive strength.....	47
Figure 4.6 (a): Interaction plots for linear shrinkage.....	48
Figure 4.6 (b): Interaction plots for water absorption.....	48
Figure 4.6 (c): Interaction plots for apparent porosity.....	49
Figure 4.6 (d): Interaction plots for bulk density.....	49
Figure 4.6 (e): Interaction plots for compressive strength.....	50
Figure 4.7 (a): Contour plot of linear shrinkage (%) vs sintering temperature, wt.% WS... 53	53
Figure 4.7 (b): Contour plot of water absorption (%) vs sintering temperature, wt.% WS... 54	54
Figure 4.7 (c): Contour plot of apparent porosity (%) vs sintering temperature, wt.% WS.. 54	54
Figure 4.7 (d): Contour plot of bulk density (g/cm ³) vs sintering temperature, wt.% WS... 55	55
Figure 4.7 (e): Contour plot of compressive strength (MPa) vs sintering temperature, wt.% WS.....	55
Figure 4.8 (a): XRD characterization of the porous ceramic 10 wt.% (850°C).....	56
Figure 4.8 (b): XRD characterization of the porous ceramic 10 wt.% (950°C).....	57
Figure 4.8 (c): XRD characterization of the porous ceramic 20 wt.% (950°C).....	57
Figure 4.9: XRD characterization of the porous ceramic.....	58

LIST OF ABBREVIATIONS

PFA	Pore Forming Agent
WS	Walnut Shell
KC	Kaolin Clay
FTIR	Fourier Transformation Infrared Spectroscopy
XRD	X-ray Diffraction
GFFD	General Full Factorial Design
ANOVA	Analysis of Variance
DSC	Differential Scanning Calorimetry

UNIVERSITI
MALAYSIA
KELANTAN

LIST OF SYMBOLS

%	Percentage
°C	Degree Celcius
2θ	Diffraction Angle
MPa	Compress Strength
g/cm^3	Bulk Density

UNIVERSITI
MALAYSIA
KELANTAN

CHAPTER 1

INTRODUCTION

1.1 Background of Study

Ceramics are considered porous if they have a high percentage of porosity, which typically ranges from 20% to 95% of the total volume (German et al., 2009, Chen et al., 2021). In the process of evaluating the porosity of a ceramic body, it is feasible to make distinctions between open porosity and closed porosity, amongst other types of porosity. The existence of either open dead-end pores or open pore channels is indicative of the permeability of the material in question (Yurkov, A., 2017). As a result of its high porosity, large surface area, strong resistance to heat, and high resistance to corrosion, porous ceramics have found significant use in a wide range of industrial sectors. These sectors include biomedical implants, hot-gas purifiers, catalyst supports, and thermal insulation (Ali et al., 2017, Zhang et al., 2022).

The method that being used in produce porous ceramic is pore-forming agent (PFA). The kind of PFA, both organic and inorganic, may have a substantial influence on the final porosity and characteristics of the ceramic material. Organic pore-forming agent may result in smaller, more uniform pores owing to regulated burning off the organic material during fire (Vogli et al., 2012, Dele-Afolabi et al., 2017, Silva et al., 2022). Recent research has investigated the viability of using food waste as an alternative PFA in the manufacture of porous ceramics. Due to their abundance and low cost, the banana stem (Sengphet et al.,

2013), rice husk (Dele-Afolabi et al., 2022), and potato starch (Eva et al., 2008) have been studied as organic PFA. These materials contain cellulose and other organic compounds that can vaporise off during the sintering process, leaving a porous ceramic substance.

This resulting material has good mechanical properties and shows potential for use in applications such as adsorption, catalysis, and insulation (Xia et al., 2022). The use of walnut shells (WS) as a PFA in porous ceramics has been the objective of this study. When contemplating the use of WS powder as a PFA in the manufacture of porous ceramics, it is recommended to aim for a moisture content between 5 and 10%. This range of moisture content is deemed desirable to guarantee the powder's suitability for its intended function. By keeping the moisture content within this optimal range, the integrity of WS powder can be maintained, allowing for its effective incorporation into ceramic mixtures. This preliminary study lays the groundwork for further investigation and experimentation with WS powder as a possible PFA in the development of porous ceramics with desirable properties.

1.2 Problem Statement

Due to the high moisture content of food waste materials such as banana stems, rice husks, and potato starch, it may be challenging to prepare these materials for use as PFA in clay-based porous ceramics. The moisture level of these materials ranges from 15.1% to 91%. This moisture concentration makes the grinding process more difficult, which is necessary since a powdered form of PFA needs to be ground into powder form. During the grinding process, an inefficient and variable powder may be formed if an excessive amount of moisture causes clumping, clogging, and an uneven distribution of particle size. This may be caused by an uneven distribution of particle size. A porous ceramic of high quality will have an appropriate balance between its open porosity and its compact strength. The moisture

content of WS ranges from a low of 6.34% to a high of 10.11%, despite the fact that WS is a by-product of the food sector (Saeed Salih, 2020). It is anticipated that porous ceramic containing particles of WS of uniform size would have consistent pore sizes and balanced features between porosity and compressive strength. As a result, this study will investigate the suitability of WS as a PFA for the production of porous ceramic.

1.3 Expected Output

The WS is an excellent material for producing porosity in ceramic objects because of its low moisture content, as well mentioned before in Section 1.2. Due to this, the wt.% of WS used in this inquiry ranges from 0% to 20%, which suggests that an increase in the weight percentage of WS will result in an increase in the porosity of the ceramic body. The pores in the ceramic structure are created as a result of the fact that WS particles are present during the sintering process. The sintering temperature must be carefully determined in order to produce a porous ceramic of good quality. The intent of this study is to determine of temperature on the porosity and microstructure of ceramic materials by subjecting them to temperatures of 850, 900, and 950 °C.

1.4 Objective

The objectives of this study are:

1. To evaluate the suitability of walnut shell as a PFA for porous ceramics.
2. To investigate the effect of wt.% walnut shell and sintering temperature on the physical and mechanical properties of porous ceramics.

1.5 Scope of Study

This study intends to determine the impact of WS on the porosity, physical and mechanical properties of porous ceramics. The investigation is conducted in two stages. In the first stage, basic materials were prepared and characterise. The walnut is purchase at a market. For the characterization procedure, the WS being prepare. Before the fabrication process, it was characterised using Fourier Transfer Infrared Spectroscopy (FTIR) and X-Ray Diffraction (XRD) to distinguish the functional group and compound existence of the unprocessed material. Physical properties, including bulk density, porosity, and water absorption, are also characterised. In addition, mechanical properties will be using the compressive strength. Then, utilising Scanning Electron Microscope (SEM) and XRD, the porous ceramic surface analysis and crystalline phase were characterised.

1.6 Significances of Study

This study will provide a fresh perspective or alternative approach to creating a porous ceramic with superior properties and reduced production costs. This study will also serve as a useful reference for future research on producing porous ceramic from WS waste with superior physical and mechanical properties by selecting the optimal weight percentage and sintering temperature. The manufactured porous ceramic will then be utilised in a variety of disciplines for specific applications.

CHAPTER 2

LITERATURE REVIEW

2.1 Introduction to Porous Ceramic

Ceramics are considered porous if they have a high percentage of porosity, which typically ranges from 20% to 95% of the total volume (Chen et al., 2021). Those pores give porous ceramics with distinctive properties and make them applicable to a variety of applications. They are suitable for filtration, catalysis, and biomedical engineering because they have a large surface area and can control pore size (Zhang et al., 2022). Due to their thermodynamic stability, chemical resistance, and mechanical strength, porous ceramics are applicable in a variety of industries. The porous material has the potential to conduct efficient filtering since it can capture and remove particles of a certain size range. The increase in both the surface area and the porosity of the structure contribute to an improvement in the catalytic activity of the material.

2.1.1 Formulation of Porous Ceramic

Porous ceramics involve raw materials, including ceramic powders, binders, and pore-forming agents. The manufacturing process typically involves shaping the ceramic mixture into a desired form, followed by sintering at high temperatures to densify the material. In addition, the strength, fracture toughness, and hardness of porous ceramics are affected by the ceramic matrix composition and production processing parameters (Pia et al., 2015). Subsequently, the next section will examine kaolin clay as one formulation in manufacturing porous ceramics.

2.1.2 Kaolin Clay

Kaolin clay, also known as China clay, is a versatile substance that has been the subject of many studies in the field of ceramics due to its use in numerous other industries, such as the ceramics, paper, and cosmetics industries. The principal mineral component of this type of porous white clay is kaolinite. Kaolin clay is in high demand due to its adaptable characteristics. The very fine particle size of kaolin clay, which ranges anywhere from 0.1 and 10 micrometres on average, is responsible for the clay's remarkable flexibility and workability. This property makes it easier to mould and mould the clay during the production process for ceramics (Kwon et al., 2023).

Kaolin is mostly composed of hydrated aluminium silicate, which has the chemical formula $\text{Al}_2\text{Si}_2\text{O}_5(\text{OH})$. It has a high concentration of alumina, which is typically between 36 and 40%, and a low proportion of iron oxide, which contributes to its white colour and excellent performance in ceramics (Akhmadiyeva et al., 2023). The temperature behaviour of kaolin clay is one of its distinguishing characteristics. The firing of kaolin clay results in the formation of a number of different phases, including mullite and cristobalite. The presence of

these phases helps to bring about the construction of a compact ceramic framework that has improved mechanical properties, such as greater strength and thermal stability (Low et al., 2017). On the other hand, kaolin clay has a high degree of chemical inertness, which makes it resistant to acid attacks and potentially useful in the production of ceramics that are chemically resistant (Liu et al., 2015). The next section will discuss WS as PFA in manufacturing porous ceramics.

2.1.3 Pore-Forming Agent (PFA)

PFAs, or pore-forming agents, are materials that combust on the fire (that are used to create pores). Organic and inorganic PFA are the two categories that make up PFA (Hübner et al., 2023). The synthesis of materials bases highly on pore-forming agents since these agents involve the formation of holes or voids inside the structure. These pores or spaces have an influence on the structure's properties, surface area, and porosity. Combining materials in an innovative and environmentally friendly approach may be accomplished through the use of organic pore-forming agents that are produced from food waste.

The study has found that the utilisation of fruit peels, which are abundant in cellulose and other polymers, is a natural source for the production of pores. Some examples of fruit peels are citrus peels and banana husks (Kumar et al., 2020). The addition of these waste materials into the compound process causes them to either burn off or break down, resulting in the formation of porous structures. When it comes to the manufacturing of porous carbon composites, for instance, citrus peel extracts have been explored for their potential as templates for pore formation and their high carbon content. This is because of the fact that they contain a lot of carbon.

On the other hand, the adaptability of the synthetic material is shown by inorganic pore-forming agents, such as polymeric templates. The ability of polymers like Pluronic block copolymers, which are well-known for their capacity to self-assemble into micelles, has been used in the production of mesoporous materials. On another hands, these polymers are used as templates in order to include pores into the final product's structure (Zhao et al.,1998). After the decomposition of these polymers, the porosity architecture that was supposed to be there is subsequently sustained.

2.1.4 Summary

One of the most important components in the production of porous ceramics is kaolin clay, which is an element that is both flexible and widely available. When combined with pore-forming agent, ceramics based on kaolin have the potential to created porosity as well as qualities that are unique to themselves. Creating an ideal porosity structure inside the ceramic matrix requires the use of pore-forming agents, which might include organic polymers, inorganic salts, or sacrificial templates. These agents play a very important role. The introduction of these agents enables the production of porous ceramics with controlled pore size, distribution, and volume, which in turn has an influence on the physical, mechanical, and functional properties of the porous ceramics that results. Ceramics based on kaolin may achieve increased surface area, better permeability, thermal insulation, and mechanical strength through the careful selection and manipulation of pore-forming chemicals. This makes them suitable for applications in the fields of study of filtration, catalysis, thermal management, and biomedical sciences.

2.2 Inorganic PFA as Production of Porous Ceramic

Inorganic materials are a diverse group of compounds distinguished by the lack of carbon-hydrogen (C-H) bonds, as opposed to organic materials, which depend on these kinds of bonds (Speight, 2017), (Ahmad, 2023). The definition of "inorganic PFA" refers to fugitive materials that are used in the production of porous ceramics that do not include carbon. Recent research has shown that a variety of inorganic PFA produced from waste from industrial processes have been used in porous ceramics. In light of this, the next paragraph will talk about a few studies that have been conducted on the use of industrial waste as an inorganic PFA for the creation of porous ceramics.

2.2.1 Types of Inorganic PFA

Inorganic pore-forming agents, most particularly of the research works focus on utilizing it based on the industrial waste in porous ceramic production. The studies have discovered an inorganic PFA that was manufactured from drinking water treatment sludge for use in the production of bricks (Tantawy and Mohamed, 2017). On the other hand, fly ash was used as an inorganic PFA and sintered with lead-zinc mine tailing to create an inorganic porous ceramic (Liu et al., 2017). According to Goel and Kalamdhad (2017), another research also applies the use of inorganic PFA in brick production. This particular study uses sludge from paper mills as its source. In light of this, the next part will be discussing regarding the organic PFAs that are used in the production of porous ceramic.

\

2.3 Organic PFA as Production of Porous Ceramic

The production of porosity in ceramic ceramics is mostly influenced by organic pore-forming agents, which are organic compounds that play a key part in the process. During the process of ceramic synthesis, these agents, which are often natural polymers or compounds, commonly contribute to the occurrence of voids or pores by assisting in the process. These organic agents, which may be natural polymers or waste materials that are rich in cellulose, lignin, or other organic components, are mixed into the ceramic matrix, and then during the sintering process, they either disintegrate, vaporise, or burn off. The properties of the porous network are determined by the characteristics of the gaps or holes that are left behind by the decomposition inside the ceramic structure. The properties of the porous ceramics that are produced as an outcome of the organic pore former has the potential to vary depending on the composition of the organic pore former and the processing applications that are used. These characteristics include greater surface area, higher permeability, improved thermal insulation, and maybe particular functionality.

2.3.1 Types of Organic PFA

Creating porous ceramics using the use of food waste as an organic pore-forming agent is a new method that is contributing to preserving the health of the environment. The use of food waste as an organic pore forming in the manufacturing of ceramics reveals its potential function in the synthesis of sustainable materials, which is in keeping with the targets of waste reduction and opens up new paths for the production of porous ceramics that are beneficial.

Coffee ground waste (Alzukaimi & Jabra, 2018) is used as PFA to make porous alumina ceramics. Nasir Fauzan, 2022, on the other hand, studied the use of peanut shell as a PFA in clay-based porous ceramics. Meanwhile, some researches have utilised banana peel as a PFA for porous ceramic (Mouiya et al., 2019). The following section will discuss the physical properties of the porous ceramic that includes coffee ground, peanut shell, and banana peel. These parameters include shrinkage, water absorption, apparent porosity, bulk density, and compressive strength.

2.4 Physical and Mechanical Properties of Porous Ceramic

The behavioural and performance characteristics of materials, especially porous ceramics, can be largely explained by their physical and mechanical properties, which serve as important abilities. One of the first physical properties that porous ceramic must possess is the shrinkage. Using these results, ceramic producers may be able to predict the appropriate mold or die size for a certain fired ware size by measuring clay or body shrinkage after drying and firing under a variety of processing circumstances (ASTM C326-09, 2018). This may be accomplished by observing the shrinkage of the clay or body after this procedure. Other essential physical properties include water absorption, apparent porosity, and bulk density. When evaluating the mechanical strength of porous ceramics, the compressive strength is a highly significant factor to consider.

2.4.1 Inorganic PFA

Presented in Table 2.1 is a comparison of the mechanical and physical properties of all of the inorganic PFA that was reviewed.

Table 2.1: Comparison of the mechanical and physical properties of all of the inorganic PFA

Inorganic PFA	Shrinkage	Water Absorption	Apparent Porosity	Bulk Density	Compressive Strength	Reference
Drinking Water Treatment Sludge (15-60 wt.% 700-1000 °C sintering temperature)	-	-	(41.0-28.0) – (38.0-4.0)	(1.61-1.71) – (1.85-1.72)	(41.19-27.46) – (30.40-24.52)	(Tantawy & Mohamed, 2017)
Fly Ash (30-70 wt.%, 1200°C sintering temperature)	-	4.3-6.9	48.33-65.6	1.38-0.93	-	(Liu et al., 2017)
Paper Mill Sludge (Alluvial soil, 5-20 wt.%, 850-900°C sintering temperature)	(5.02-4.12) – (5.14-4.38)	(18.0-30.0) – (17.0-29.0)	(21.0-31.0) – (20.0-31.0)	(1.23-1.03) – (1.27-1.06)	(13.5-1.5) – (16.0-1.5)	(Goel & Kalamdhad, 2017)

According to the Table 2.1, Tantawy and Mohamed, 2017 have incorporated that the incorporation of the sludge from the treatment of drinking water helps to optimise and balance the physical and mechanical properties of the ceramic brick. In order to fulfil the requirements of the brick manufacturing standard, the recommended weight percentage is between 15 and 30 %. Therefore, Liu et al., 2017 reported that 60 wt.% of fly ash used as a PFA for porous ceramic obtained good porosity and bulk density. The chemical stability of the ceramic has been increased as a result of the incorporation of fly ash. Additionally, Goel & Kalamdhad, 2017 discovered that the ideal amount of paper mill sludge to add as a PFA to alluvial soil for brick manufacture was 10 wt.%. This was done at a sintering temperature of 900 °C. In the case that the increase wt.% of the PFA is applied, the compressive strength and water absorption will decrease, making the material unsuitable for use in the manufacturing of bricks industry.

2.4.2 Organic PFA

Presented in Table 2.2 is a comparison of the mechanical and physical properties of all of the organic PFA that was reviewed.

Table 2.2: Comparison of the mechanical and physical properties of all of the organic PFA

Organic PFA	Shrinkage (%)	Water Absorption (%)	Apparent Porosity (%)	Bulk Density (g/cm ³)	Compressive Strength (MPa)	Reference
Coffee Ground (12.5-50 wt.%, 1500 °C sintering temperature)	Increase with the increase of the coffee ground content (around 68.5% for 50 wt.%)	-	35-54	42.7-5.8	-	(Alzukaimi & Jabra, 2019)
Peanut Shell (0-20 wt.%, 850-950 °C sintering temperature)	Increase with the increase of the peanut shell content	28-26	27-38	1.8-1.4	93-104 (10wt.%) 69-91 (20wt.%)	(Nasir Fauzan, 2022)
Banana Peel (20 wt.%, 900-1100 °C sintering temperature)	-	-	47.4-40.2	1.43-1.55	-	(Mouiyah et al., 2019)

Due to Table 2.2, a study has come to the conclusion that coffee waste might be used to produce porous alumina ceramics (Alzukaimi and Jabra, 2019). These ceramics have a remarkable mechanical strength of more than 17 MPa and a high porosity of up to 54%.

Through the observation, the compressive strength values of clay-based porous ceramic made from peanut shell waste (Nasir Fauzan, 2022) remained very high (ranging from 93.22 to 104.39 MPa for 10 wt.% and from 69.65 to 91.62 MPa for 20 wt.%). In addition to the high porosity percentage in the porous ceramic with 10 wt.% and 20 wt.% of the peanut shell, this has shown that the Mohs hardness of each crystalline phase that is present in the porous ceramic helps to increase its compressive strength. Besides that, the strength of the porous ceramic that was incorporated into the banana peel was significantly improved when the sintering temperature was increased from 900 to 1100° C (Mouiya et al., 2019). It has come to the conclusion that a sintering temperature of 1100° C is necessary in order to attain an ideal balance between porosity (40.2% of the total) and strength (8 MPa).

2.4.3 Summary

When compared to inorganic PFA, organic PFA that is centred on food waste has various benefits in terms of combustibility, toxicity, and cost-effectiveness. This conclusion can be drawn from the organic PFA part that has been previously discussed. A thorough investigation of the chemical composition and physical properties of the porous ceramic that will have an effect on its performance is required, however, before the walnut shell can be used as a PFA. This research will focus only on PFA from the solid waste industry. The PFA will be further discussed in Section 2.5.

2.5 Walnut Shell

Walnut shell is a natural material that is obtained from the exterior shell of walnuts (*Juglans regia L*), which is also referred to as the husk in certain instances. As a result of its unique characteristics and malleability, it is used extensively in a broad variety of domains and contexts. One characteristic that sticks out about WS is its level of hardness. Due to the fact that it has a hardness of around 3.5 on the Mohs scale, it is beneficial in environments that are abrasive. The WS has a level of hardness that makes it suitable for use as an abrasive media in a range of contexts, including the metal finishing industry, the automobile industry, and the aerospace industry (Abdullah et al., 2014, Beskopylny et al., 2023).

Despite its hard exterior, the WS has a naturally permeable structure. Because the natural structure of the shell consists of tiny holes and voids, it may be used as a PFA in ceramics, as well as for filtration and absorption purposes in many contexts. Due to the fact that WS is porous, it may be used for a variety of functions, such as filtering water and absorbing oil. The porous nature of a WS gives it extraordinary water-adsorption qualities. The shell's interconnected voids and channels contribute to its high porosity, which in turn provides a large surface area for water adsorption. Because of this, WS can hold a lot of water despite its relatively modest weight. It can absorb large amounts of water, making it useful in many applications. The researcher found that the specific surface area of the adsorbent grew from 1076 to 1434 m²/g, while the average pore diameter reduced from 3.23 to 2.08 nm and the total pore volume decreased from 0.86 to 0.74 m³/g. This resulted in a significant improvement in the morphology of the adsorbent (Albatrni et al., 2022). Additionally, WS can be used as an element in the production of porous ceramics, which can be utilised in a broad variety of industrial settings (Gong et al., 2012). In addition to this, WS is a material that is both renewable and sustainable. As a standard practise, the walnut

business either disposes of the shells or finds another use for them as a by-product. WS may be used instead of other materials that need more resources and are more wasteful, which is beneficial to the environment.

2.5.1 FTIR Analysis of Walnut Shell

Before using the walnut shell to make a new material, it is essential to do FTIR analysis in order to identify the functional groups that are present in the walnut shell (including cellulose, lignin, hemicellulose, protein, and ash) (Uddin & Nasar, 2020). Figure 2.1 shows of the FTIR peak of the walnut shell.

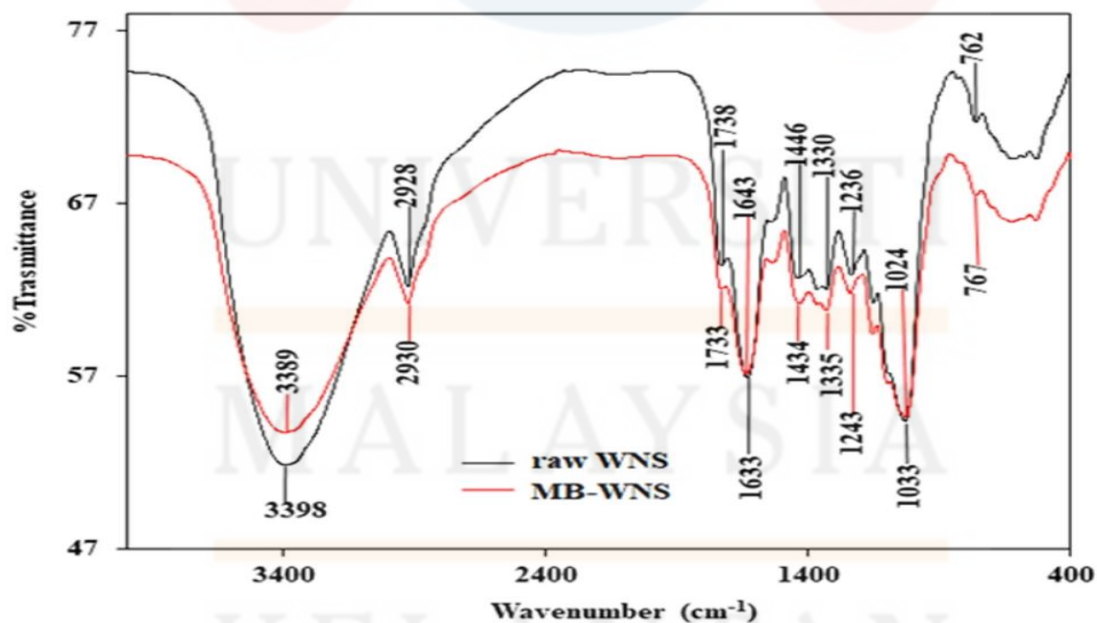


Figure 2.1: FTIR peak of walnut shell (Uddin & Nasar, 2020)

Figure shows large peaks of raw WS (black line) in the functional group area at 3398, 2928, and 1633 cm^{-1} . The peak at 3398 cm^{-1} is due to O-H stretching vibration, whereas 2930 cm^{-1} is due to C-H stretching vibration of alkane. The band at 1738 cm^{-1} is caused by C=O stretching of the carbonyl group, whereas the band at 1633 cm^{-1} might be due to C=C stretching of alkene or N-H bending of amine. It is necessary to conduct the review in order to compare the FTIR results of the walnut shell that will be used in this project.

2.6 Overall Summary

The use of WS as a PFA in the producing of porous ceramics has been attracting a great deal of interest. In order to achieve desired qualities such as low density, high surface area, and increased thermal insulation, porous ceramics have a network of interconnected voids or pores. Since WS are cheap, renewable, and plentiful, they may be used to make porous ceramic structures. Modifying the particle size of the WS, the concentration of the WS in the ceramic mixture, and the sintering temperature all have a role in determining the pore size, shape, and distribution. These factors, when optimized, allow for the porosity and pore properties to be tailored to the needs of the specific application.

CHAPTER 3

MATERIALS AND METHODS

3.1 Research Flow

The research flowchart will consist of two stages as shown in Figure 3.1 and Figure 3.2.

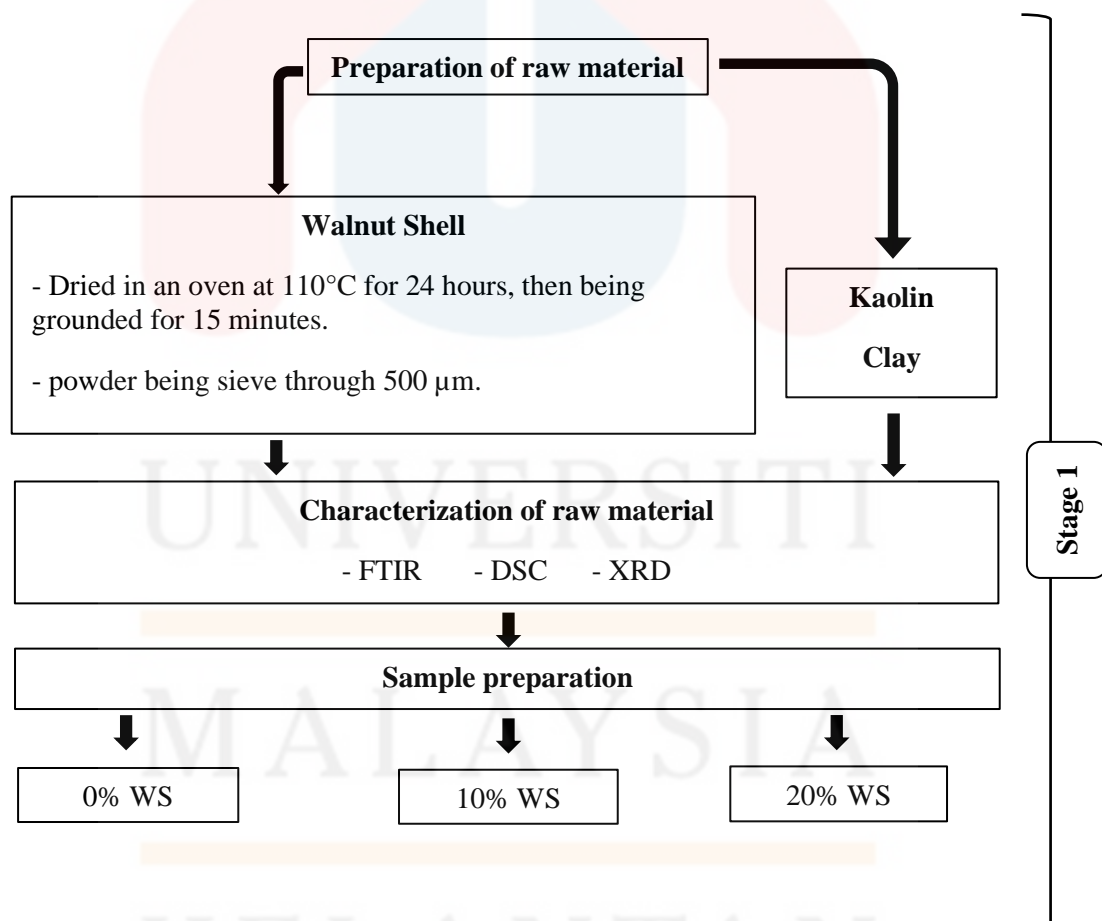


Figure 3.1: Research flow stage 1 for porous ceramic incorporated with WS.

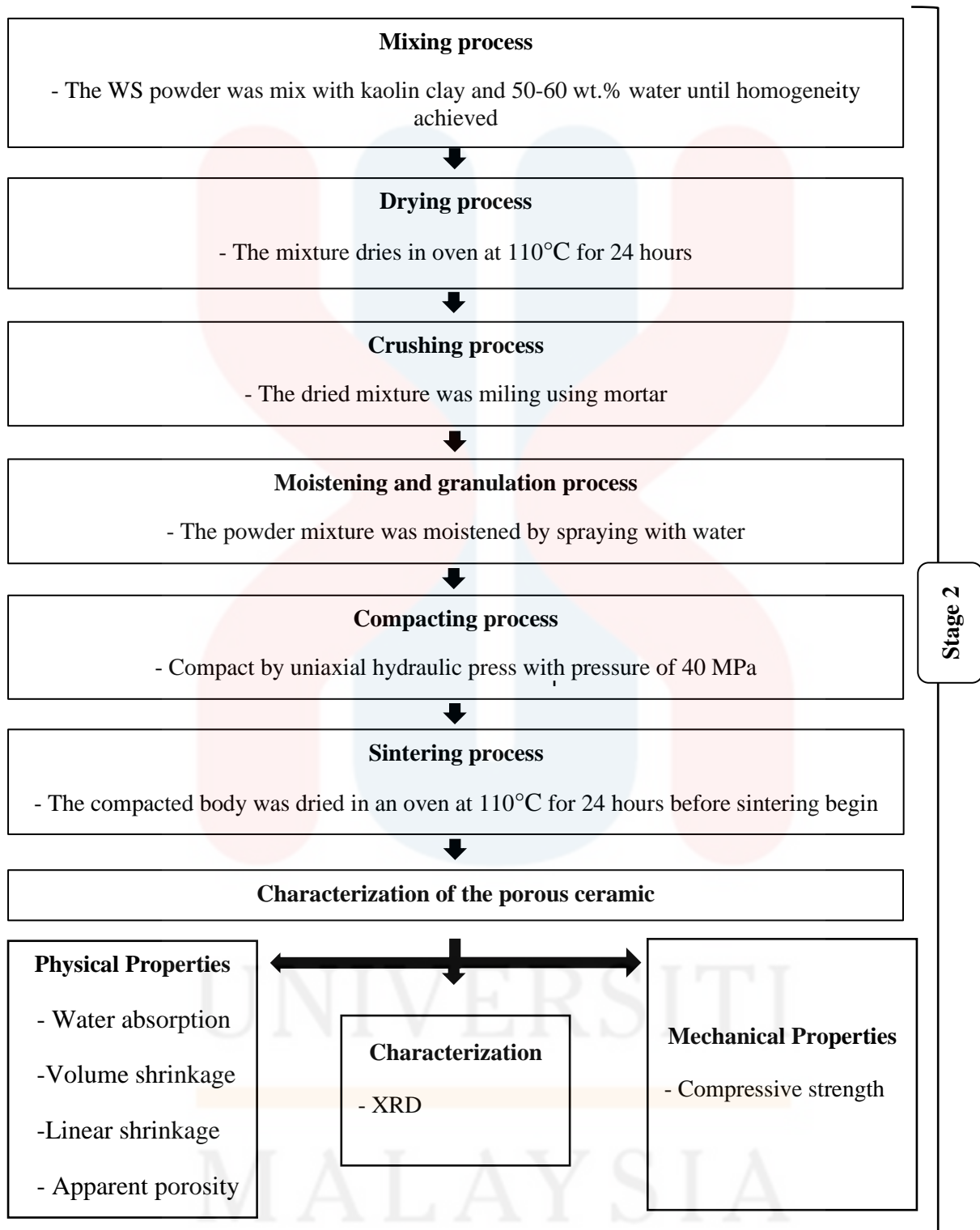


Figure 3.2: Research flow stage 2 for porous ceramic incorporated with WS.

3.2 Materials

3.2.1 Walnut Shell

The WS was dry in an oven for 24 hours at 110 °C. The amount of moisture was determined by comparing the mass before and after the test. The dried WS was chopped and ground in a high-speed processor and grinder for 15 minutes. Powdered WS will be sieved through a 35-mesh, 500 µm test sieve to remove larger particulates for the ASTM E11-16 compliant porous ceramic. Afterwards, a model iZ10 equipped with FTIR analysis will be used to examine the functional group of the WS powder using wavenumbers between 600 and 4000 cm⁻¹.

3.2.2 Kaolin Clay

The clay for the undertaking were supplied by Kaolin (Malaysia) Sdn. Bhd., a local manufacturer. This clay's white colour and malleability are a result of the mineral kaolinite present within it. Therefore, kaolin clay and WS were mix to create a porous ceramic. The kaolin clay is characterize using XRD and DSC. In addition, the crystalline phase of kaolin clay will be characterised by XRD using a Bruker Model D2 Phaser and CuK α radiation ($\lambda=1.5418$ Å) in the range of $2\theta=10^\circ - 90^\circ$.

3.3 Methods

The production of porous ceramic using WS as a PFA involves several steps. First, the WS must be collected and dried completely to remove moisture. The dried shell was grounded using grinder and sieved through 500 µm siever to produce a fine powder with particle size 500 µm and below.

Next, kaolin clay and the grinded WS particles are combined with 50-60 wt.% water for one hour. The WS being add in varied at 0, 10, 20 wt.%. The mixture then dries in an electric oven at 110°C for 24 hours. In order to produce the powder mixture and re-homogenize the composition, the dried mixture was milled for one hour using mortar.

The powdered mixture was subsequently granulated, which was the next step in the procedure. The powder was first being spray with distilled water using a spray bottle in order to moisten it. The amount of moisture to be added to the powder mixture is between 5 and 6 wt.%, or 5 to 6 g per 100 g of powder. According to ASTM E11-16, the moist powder then being passing through a test sieve with 60 meshes and a 250 μm opening size to generate granule powder. The granule powder being press using a uniaxial hydraulic press with a pressure of 40 MPa in a hardened tool steel mould, yielding a green body of 20 mm in diameter. Before being heated for one hour in a muffle furnace, the compressed body was dried out in a 110 °C electric oven for 24 hours. After the material has been thoroughly dried, it is ready to be sintering. Typically, the sintering process is conduct at three temperatures: 850, 900, and 950 °C. During the sintering process, the WS particles are consume, leaving the ceramic matrix with holes. In addition to undergoing sintering, the ceramic particles will unite to form a solid structure.

After the sintering has concluded, the porous ceramic is cooled slowly to prevent thermal stress. After that, it can be examined for physical properties. Porous ceramic samples will be put in test for water absorption, linear shrinkage, and apparent porosity and bulk density.

3.3.1 Water Absorption Characterization

The porous ceramic sample's water absorption was characterised by the use of the MS ISO 10545-3:2001 standard in this research. Calculations will be carried out to determine the sample's apparent porosity, bulk density, and rate of water absorption. Before the sample is weighed, the dry mass of the sample will first be acquired using the vacuum method in order to calculate the amount of water that can be absorbed by the sample. The method involves removing air out of a chamber containing samples. The samples will be taken out of the water after being submerged for 30 minutes at room temperature. After being washed, the sample will be patted dry before being reweighed to determine the amount of cold water that has saturated its entire mass. After being completely submerged in water, the sample will go through another round of weighing. For the purpose of determining the volume (V) of each sample, the water displacement process will be used. Using the following equation, it will determine the apparent porosity, relative density, and bulk density of the samples, both before and after the sample have been submerged in water.

$$E(v) = (m^2(v))/m^1 \times 100$$

Equation 1

Where:

m^1 : mass of dry porous ceramic.

m^2 : mass of wet porous ceramic.

v : volume.

Apparent Porosity (P)

$$P = (m^2/v) - m^1/v \times 100$$

Equation 2

Where:

m^1 : mass of dry porous ceramic.

m^2 : mass of wet porous ceramic.

v : volume.

Bulk Density Equation (B)

$$B = m^1/v$$

Equation 3

Where:

m^1 : mass of dry porous ceramic.

v : volume.

In the calculations that will be done in the future, 1 cm³ of water will be considered to equal 1g. This is accurate to within 3% when measured at room temperature.

3.3.2 Linear Shrinkage

The linear shrinkage will be determined using ASTM C326-09, 2018, as the standard.

The following formula is provided for calculating the linear shrinkage of the sample:

$$St = \frac{Lp - Ld}{Lp} \times 100$$

Equation 4

Where:

St: total linear shrinkage after drying and firing, %.

L_p: plastic length of the test specimen.

L_d: fired length of the test specimen.

3.3.3 Compressive Strength

In order the purpose of compressing the porous ceramic, a testometric universal testing machine will be used. For the intention of determining the strength of a sample that has been measured using a testometric universal testing machine with a test speed of 0.1 mm/min and a preload of 5 N, the following formula is used.

$$F = \frac{P}{A} \quad \text{Equation 5}$$

Where:

F: compressive strength (N/mm²)

P: applied load (N)

A: surface area (mm²)

3.3.4 XRD Analysis

The crystalline phase in the porous ceramic that is being characterised by XRD using a Bruker Model D2 Phaser in the range $2\theta=10^\circ - 90^\circ$ with $\text{CuK}\alpha$ radiation ($\lambda=1.5418 \text{ \AA}$).

Tablets will be the shape that the porous ceramic that has been characterised takes.

3.3.5 Fourier Transform Infrared Spectroscopy (FTIR)

FTIR analysis was used in order to accomplish its objective of determining the classification of the functional group that was present in the WS. The morphology of the porous ceramic was analysed with the use of FTIR.

3.3.6 Differential Scanning Calorimetry

In addition to identifying the connection between temperature and time that is present in the WS, the DSC analysis is important for evaluating how the physical characteristics vary over time. DSC analysis is also necessary for understanding how the conditions change over time. Temperature range and air or N₂ atmosphere are the factors that comprise the DSC. The relevance of this phase comes in the fact that it will interact with the clay and have an influence on the physical and mechanical characteristics of the porous ceramic. This interaction will contribute to the importance of this phase.

3.4 General Full Factorial Design (GFFD)

One of the methods is the design of experiment (DOE) methodology, which is often referred to as the general full factorial design (GFFD). The investigation of the key influences and interactions of variables (the parameters that are being examined) that are being performed at a variety of various levels is the primary purpose of this study. The design of this research was intended to investigate the effects of weight percentage of WS (3 levels: 0wt%, 10wt%, and 20wt%) and sintering temperature (3 levels: 850°C, 900°C, and 950°C) on the final qualities of the ceramic tile that was combined with WS. The statistical software programme MINITAB 16 was used to carry out this research. An analysis of variance (ANOVA), a normality probability plot, a residual versus fits plot, a main effects plot, an

interaction plot, and a contour plot were some of the statistical analyses that were going to be carried out in the experimental design. Additionally, a contour plot was going to be carried out. The Table 3.1 has shown the experimental design for central composite design.

Table 3.1: Experimental design matrix for general full factorial design (GFFD)

Factor			Response				
Run Oder	Wt.% WS	Sintering Temperature	Linear Shrinkage (%)	Water Absorption (%)	Apparent Porosity (%)	Bulk Density (g/cm ³)	Compressive Strength (MPa)
1	2	2					
2	1	2					
3	3	1					
4	2	2					
5	3	1					
6	2	3					
7	1	1					
8	3	3					
9	1	3					
10	1	1					
11	1	2					
12	2	1					
13	1	3					
14	2	3					
15	3	2					
16	3	3					
17	3	2					
18	2	1					

CHAPTER 4

Result and Discussion

4.1 Characterization of Raw Material.

4.1.1 FTIR Analysis of Walnut Shell

FTIR analysis is required in order to determine the identity of the functional group that is present in the walnut shell. The FTIR analysis of the walnut shell is shown in Figure 4.1.

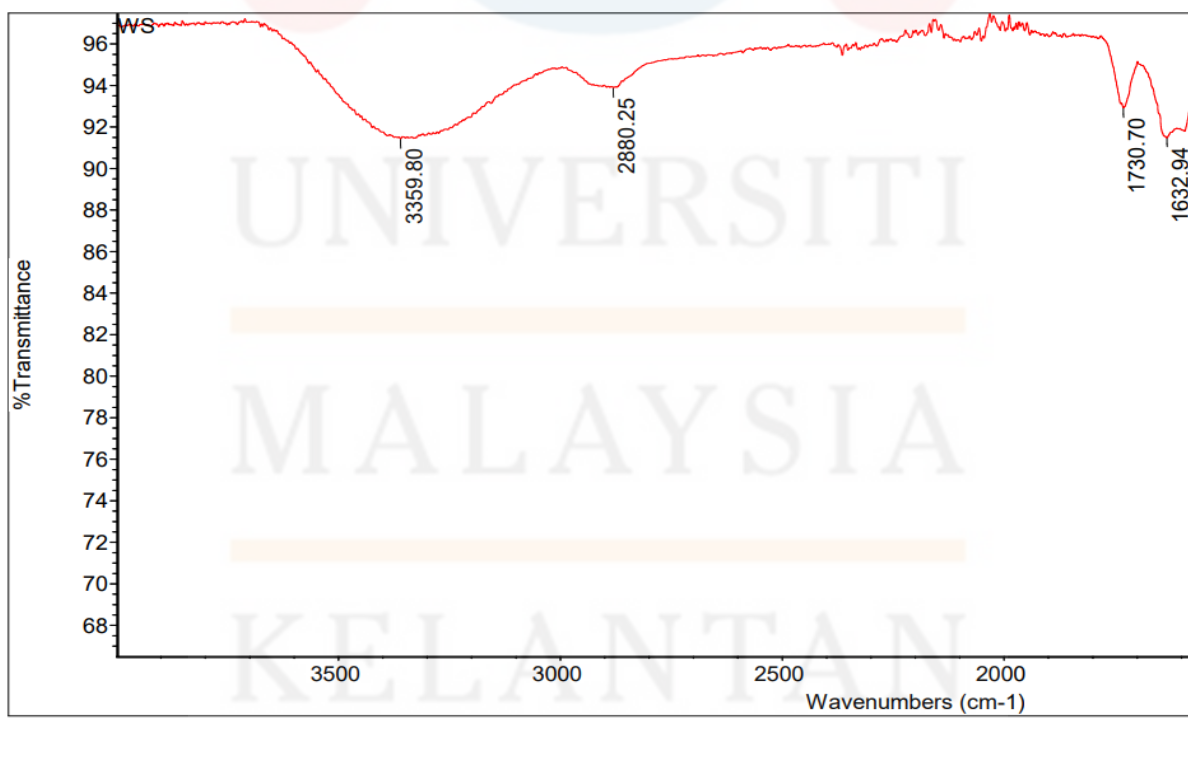


Figure 4.1: FTIR pattern of walnut shell powder.

Based on the Figure 4.1, the peak at 3359.80 represents O-H stretching vibrations in hydroxyl groups (alcohols). This peak may be attached to aliphatic primary alcohols, as well as cellulose and hemicellulose, which are rich in walnut shell composition. The peak at 2880.25 represents the C-H stretching vibrations in alkyl groups. This peak is related with aliphatic hydrocarbons found in various components of the walnut shell, such as fatty acids and wax. Meanwhile, the peak at 1730.70 was identified as the functional group of C=O stretching vibrations in carbonyl groups. This peak indicates the presence of ester carbonyls in hemicellulose or acetyl groups in lignin, both components of the walnut shell. On the other side, at the peak 1632.94, there are C-C aromatic stretching vibrations in aromatic rings. This peak is not present in aliphatic hydrocarbons or primary aliphatic alcohols. It is suggestive of lignin, which is an important component of the walnut shell structure. According to the observations, the peak in this FTIR study is quite similar to the FTIR analysis described in the literature review (Uddin & Nasar, 2020). This shows that the peanut shell was using in this study has similarities to that used in the previous study.

4.1.2 XRD Analysis of Kaolin Clay

XRD analysis is required in order to determine the major crystalline phase that is present in the walnut shell at high sintering temperatures. This phase will react with the clay, which will have an effect on the physical and mechanical properties of the resulting porous ceramic. Figure 4.2 shows an XRD analysis of raw kaolin clay.

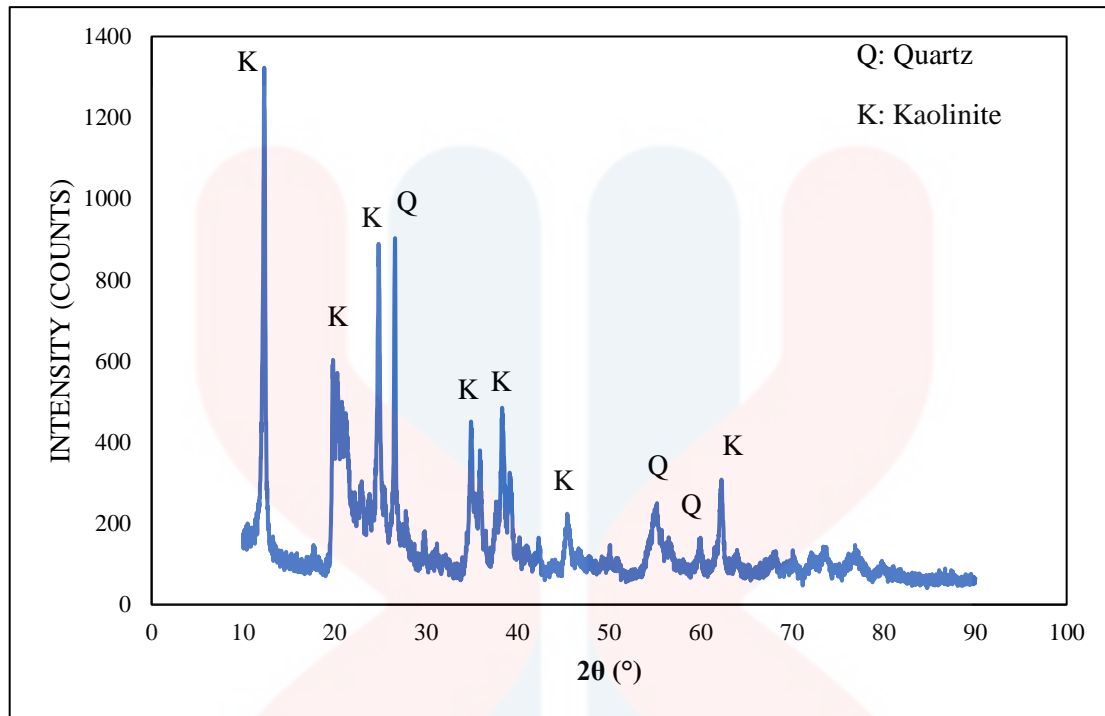


Figure 4.2: XRD analysis of raw kaolin clay.

It can be shown in Figure 4.2 that the raw kaolin clay was composed of just two different kinds of minerals, namely kaolinite (COD9009230) and quartz. Because of its chemical composition and the mineralogical features, it has, kaolin is very refractory and has a restricted flexibility even when it comes to porous ceramic. Furthermore, the crystalline phase of kaolin results in thermal properties that enable for sintering to take place at temperatures that are substantially lower than those of other ceramic materials such as alumina (Hubadillah et al., 2018). The peak in this XRD research is pretty comparable to the one that was mentioned in the literature review (Akbari et al., 2021). This is the conclusion that can be drawn from the findings. This indicates that the raw kaolin that was used in this investigation is comparable to the kaolin that was used in the previous study.

4.1.3 DSC Analysis of Ceramic Mixture

The DSC analysis is the measurement of how the physical properties change over time, in addition to the temperature versus time that is included in the WS. The significance of this phase lies in the fact that it will interact with the clay and have an effect on the physical and mechanical properties of the porous ceramic. As can be seen in Figure 4.3 (a) to Figure 4.3 (d), the DSC analysis of the raw WS powder, 0% of WS, 10% of WS, and 20% of WS is shown.

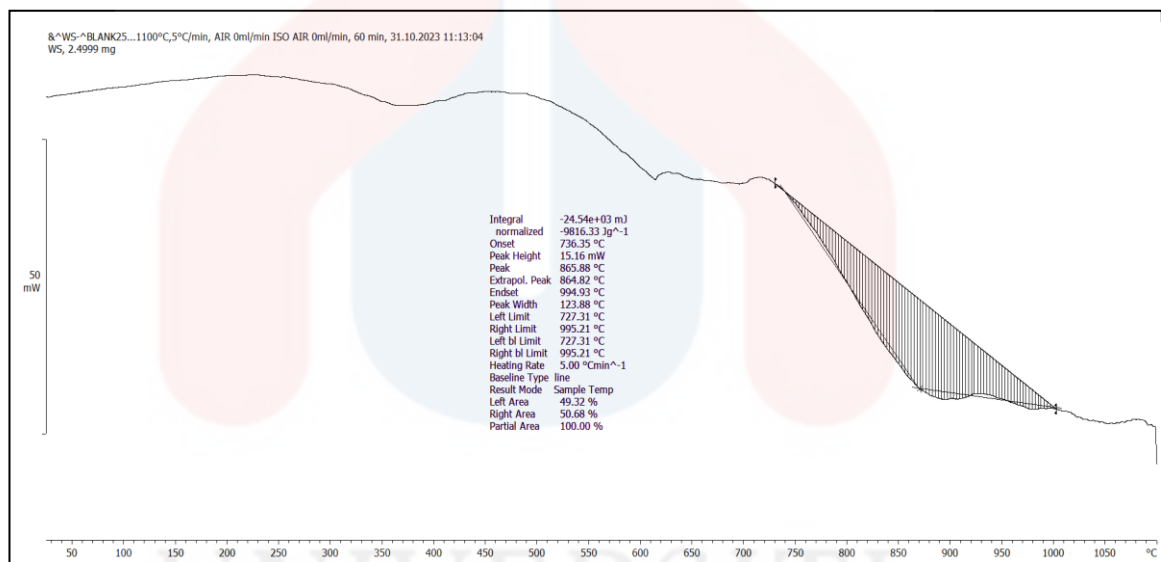


Figure 4.3 (a): DSC analysis for raw WS powder

As shown in Figure 4.3 (a), the onset began at a temperature of 736.35°C. At a temperature of 864.82°C, the raw WS is heating up entirely, and at 994.93°C, it no longer heats up at all. While heating the porous ceramic process at temperatures of 850°C, 900°C, and 950°C, the raw WS was used for kaolin clay that consumed 0 wt.%, 10 wt.%, and 20 wt.% of WS. The purpose of this experiment was to observe the impact of different temperatures had on the properties of the porous ceramic.

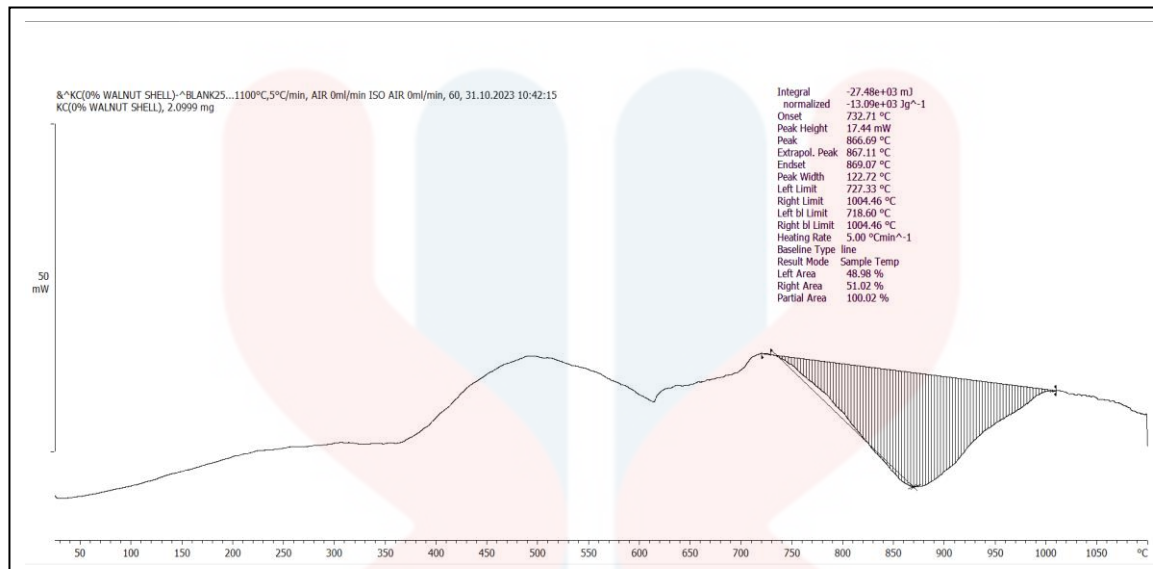


Figure 4.3 (b): DSC analysis for powder mixture incorporated with 0wt.% WS.

As can be seen in Figure 4.3 (b), the onset started at a temperature of 732.71°C. At a temperature of 867.11°C, the 0 wt.% WS is completely heating up, and at a temperature of 869.07°C, it is no longer heating up at all. The porous ceramic process was heated to temperatures of 850°C, 900°C, and 950°C using this composition. The purpose of this experiment was to determine the impact that the different temperatures possessed on the properties of porous ceramic.

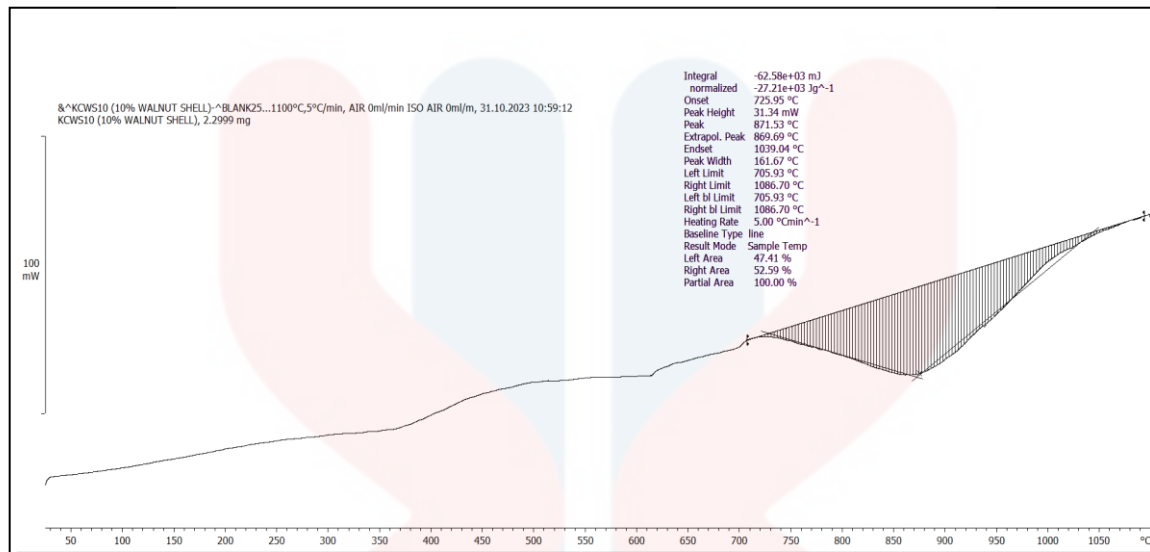


Figure 4.3 (c): DSC analysis for powder mixture incorporated with 10wt.% WS.

For the Figure 4.3 (c), the onset started at a temperature of 725.95°C. At a temperature of 869.69°C, the 10 wt.% WS is completely heating up, and at a temperature of 1039.04°C, it is no longer heating up at all. The porous ceramic process was heated to temperatures of 850°C, 900°C, and 950°C using this composition. The purpose of this experiment was to determine the impact that the different temperatures possessed on the properties of porous ceramic.

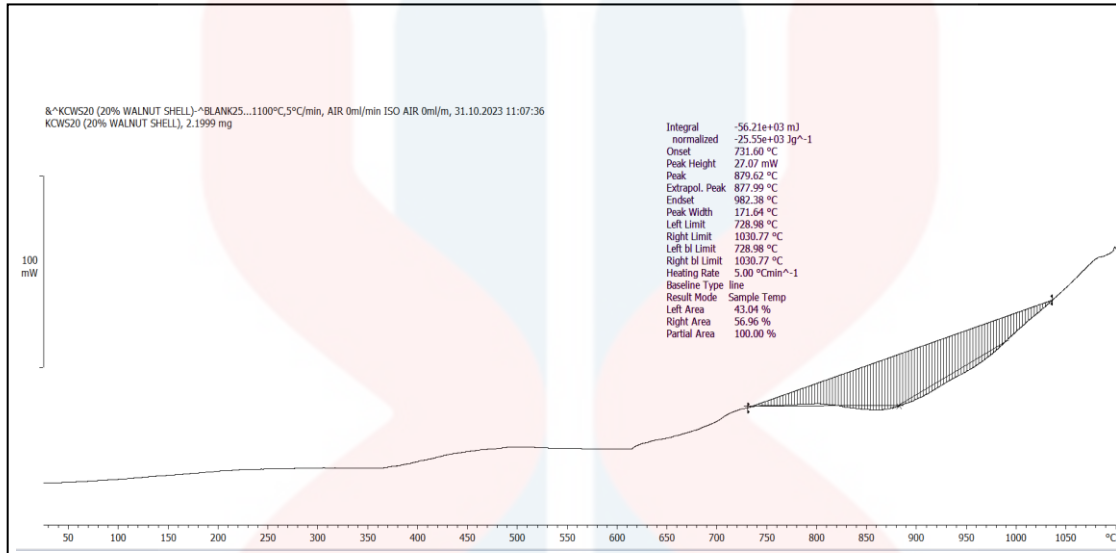


Figure 4.3 (d): DSC analysis for powder mixture incorporated with 20wt.% WS.

As can be seen in Figure 4.3 (d), the onset started at a temperature of 731.60°C. At a temperature of 877.99°C, the 0 wt.% WS is completely heating up, and at a temperature of 982.38°C, it is no longer heating up at all. The porous ceramic process was heated to temperatures of 850°C, 900°C, and 950°C using this composition. The purpose of this experiment was to determine the impact that the different temperatures possessed on the properties of porous ceramic.

4.2 General Full Factorial Design

A general full factorial design with two independent variables or operating factors was utilised in order to statistically investigate the effects of various operating factors and their interactions on predicted responses or properties of porous ceramic that was incorporated with the WS. These properties included water absorption, apparent porosity, bulk density, and compressive strength. Both the weight percentage (wt.%) of WS and the sintering temperatures were considered independent variables. These variables were indicated by the parameter's 'A' and 'B', respectively. There are three different values that may be assigned to the weight % of WS (Factor A), and these values are represented by the coded numbers one, two, and three accordingly. The temperatures at which the sintering process was carried out (Factor B) were separated into three different levels, which were represented by the numerical values 1, 2, and 3. The components that were explored in the general complete factorial design are shown in Table 4.1, together with the number of levels that were assigned to each component. Water absorption, apparent porosity, bulk density, and compressive strength were the properties that were evaluated in terms of responses with the material.

UNIVERSITI
MALAYSIA
KELANTAN

4.2.1 Experimental Design Matrix

The experimental design matrix and the experimental responses obtained from the total of 18 experimental runs that were carried out in a random order with two applications are provided in Table 4.1. These runs were carried out with two applications each. Coding was used to indicate the degree or range of each analysed component on a common scale consisting of 1, 2, and 3 for factor A and 1, and 2 for factor B, as previously reported. After that, a number of statistical analyses were carried out for each respond. These analyses included determining whether or not the model was accurate, doing an analysis of variance (ANOVA), plotting the main effects and interactions, and drawing contour plots.

Table 4.1: Experimental design matrix for general full factorial design (GFFD).

Factor			Response				
Run Oder	Wt.% WS	Sintering Temperature	Linear Shrinkage (%)	Water Absorption (%)	Apparent Porosity (%)	Bulk Density (g/cm ³)	Compressive Strength (MPa)
1	2	2	0.68560	23.1593	32.4106	1.39946	43.708
2	1	2	0.53948	18.0390	30.7575	1.70505	107.627
3	3	1	0.44226	40.0463	46.8042	1.16875	19.519
4	2	2	0.68695	23.2652	32.5433	1.39880	44.371
5	3	1	0.46614	40.7957	47.1189	1.40596	20.361

6	2	3	1.52445	24.3450	34.4616	1.41556	41.874
7	1	1	0.51584	17.0720	29.1286	1.70622	71.290
8	3	3	1.81818	39.6467	47.9006	1.20819	27.655
9	1	3	1.34837	19.3744	33.6066	1.73458	114.994
10	1	1	0.58881	17.1750	29.1472	1.69707	73.501
11	1	2	0.51559	18.4304	31.1306	1.68909	112.203
12	2	1	0.44042	20.8917	29.5922	1.41646	43.637
13	1	3	1.37423	19.5923	33.3469	1.70204	131.257
14	2	3	1.54336	24.9383	35.0289	1.40462	44.100
15	3	2	0.66274	41.6667	48.3221	1.15973	25.750
16	3	3	1.86503	39.8901	47.8321	1.19910	29.902
17	3	2	0.68949	42.2050	48.5149	1.14950	27.360
18	2	1	0.49152	21.6843	30.4873	1.40596	43.674

*For factor 'A' (wt.% of WS), '1', '2', and '3' represent 0wt.%, 10wt.%, and 20wt.%, respectively.

For factor 'B' (sintering temperature), '1', '2', and '3' represent 850°C, 900°C and 950°C respectively.

4.2.2 Model Adequacy Checking

According to Ter Teo et al. (2021), right before doing further statistical analysis, a model adequacy checking was carried out in order to examine a large number of residual assumptions. As a general rule, residuals may be described as the difference between the actual response value and the predicted response value in the field of statistics. In this particular case, the actual response values were obtained from the result of the experiment (which was shown earlier in Table 4.1, while the predicted response values were obtained from the equation that was used for regression analysis. It is the responsibility of the sufficiency verification to examine three residual assumptions: (i) residual normality, (ii) residual constant variant, and (iii) residual independence. In the event that these assumptions are correct, the regression model that is produced by the equation will be a reasonably accurate representation of the actual experimental data (Ahmad, 2023). Statistical residual plots, such as the normal probability plot residual, the histogram of frequency vs residual, the plot of residuals versus fitted or predicted values, and the plot of residuals in time sequence or observation order, are some examples of the types of plots that may be used to verify the three assumptions.

Figures 4.4 (a), 4.4 (b), 4.4 (c), 4.4 (d), and 4.4 (e) show the residual plots for linear shrinkage, water absorption, apparent porosity, bulk density, and compressive strength of clay-based ceramics that incorporate WS. These plots are shown in the figures.

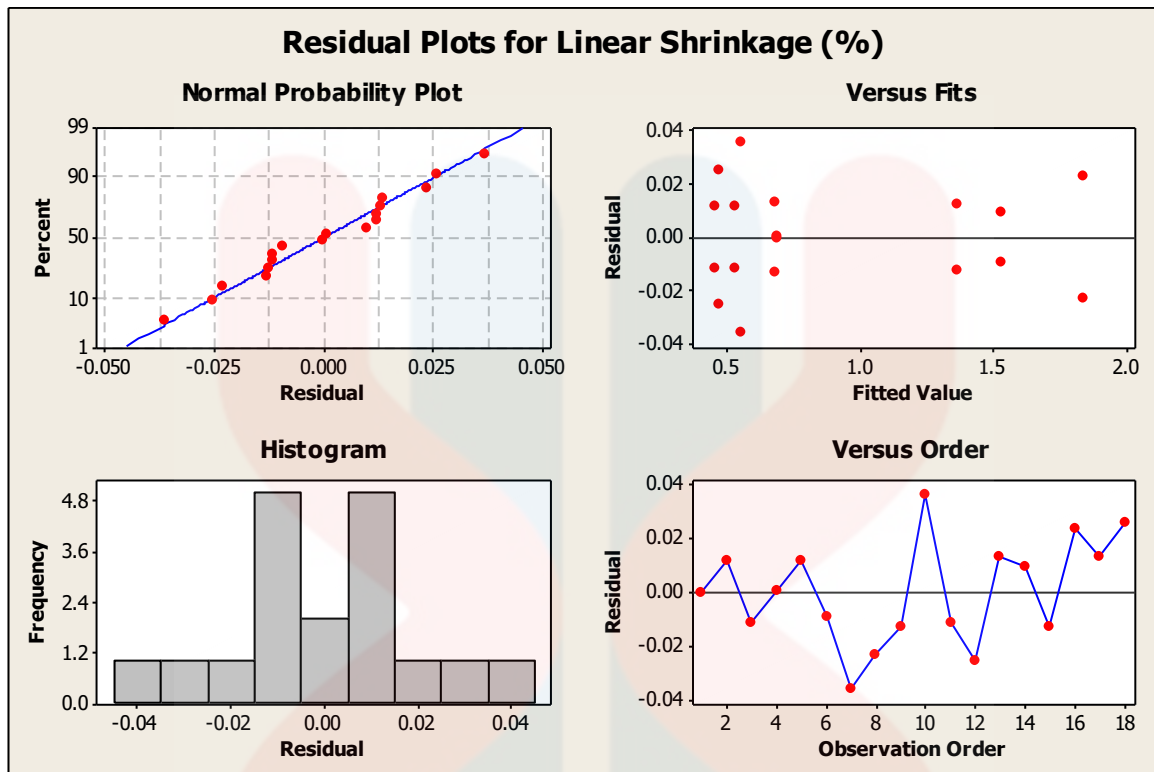


Figure 4.4 (a): Residual plots for linear shrinkage; (i) Normal probability plot, (ii) Histogram of frequency versus residual, (iii) Residual versus fits, (iv) Residual versus observation order of data

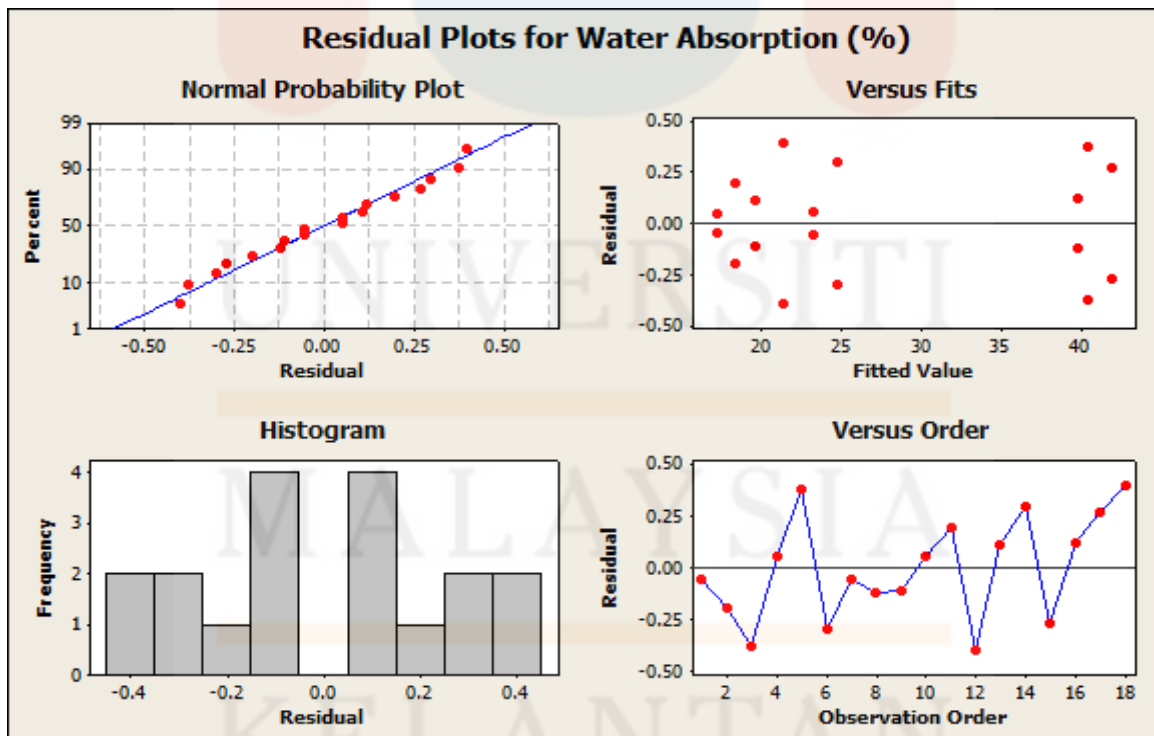


Figure 4.4 (b): Residual plots for water absorption; (i) Normal probability plot, (ii) Histogram of frequency versus residual, (iii) Residual versus fits, (iv) Residual versus observation order of data

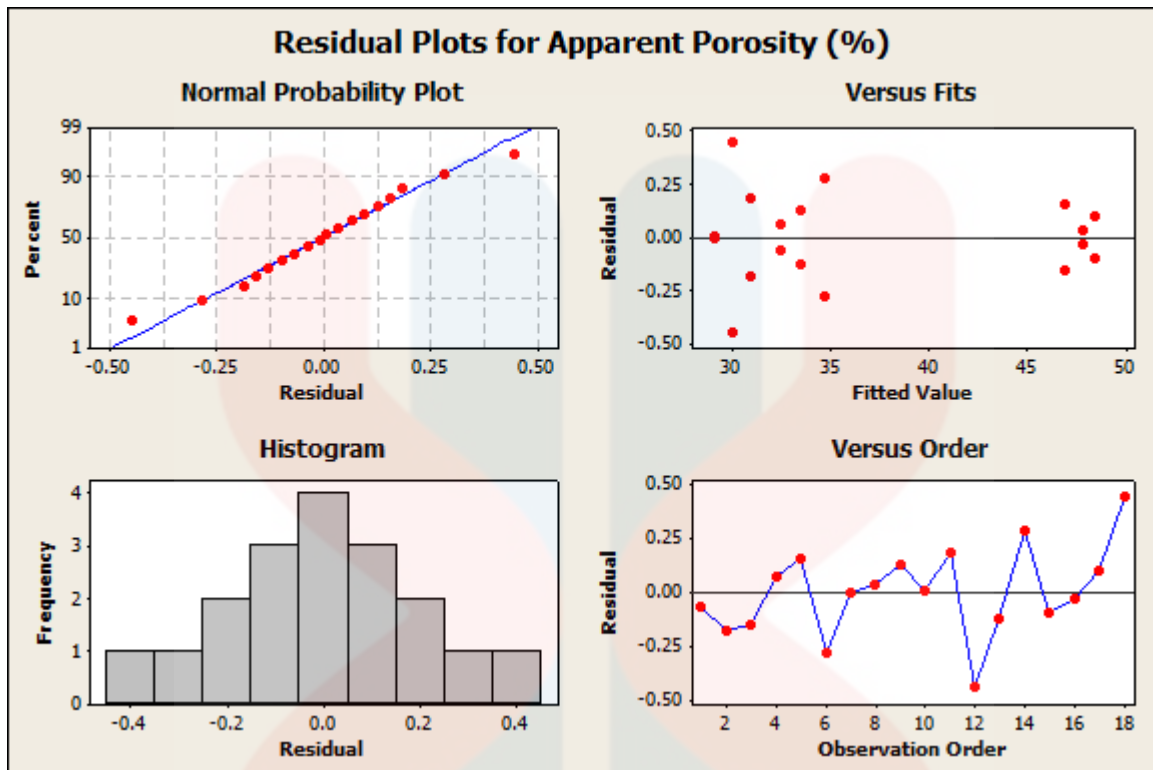


Figure 4.4 (c): Residual plots for apparent porosity; (i) Normal probability plot, (ii) Histogram of frequency versus residual, (iii) Residual versus fits, (iv) Residual versus observation order of data

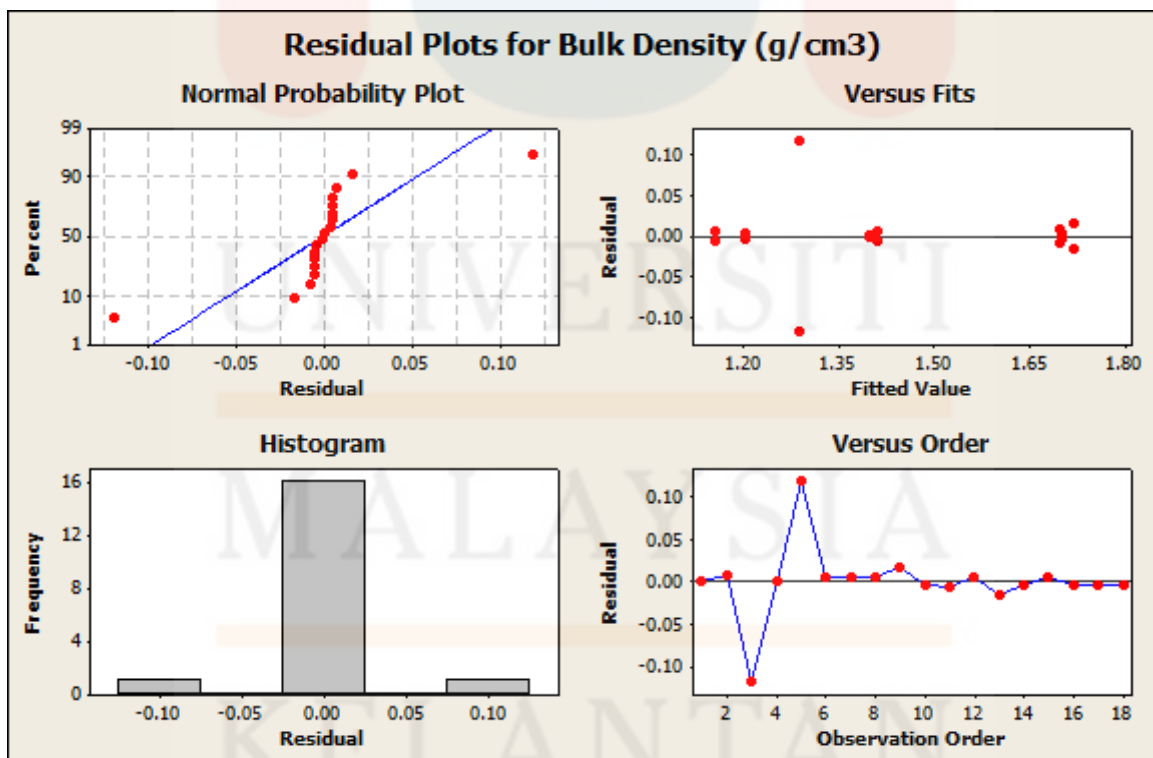


Figure 4.4 (d): Residual plots for bulk density; (i) Normal probability plot, (ii) Histogram of frequency versus residual, (iii) Residual versus fits, (iv) Residual versus observation order of data

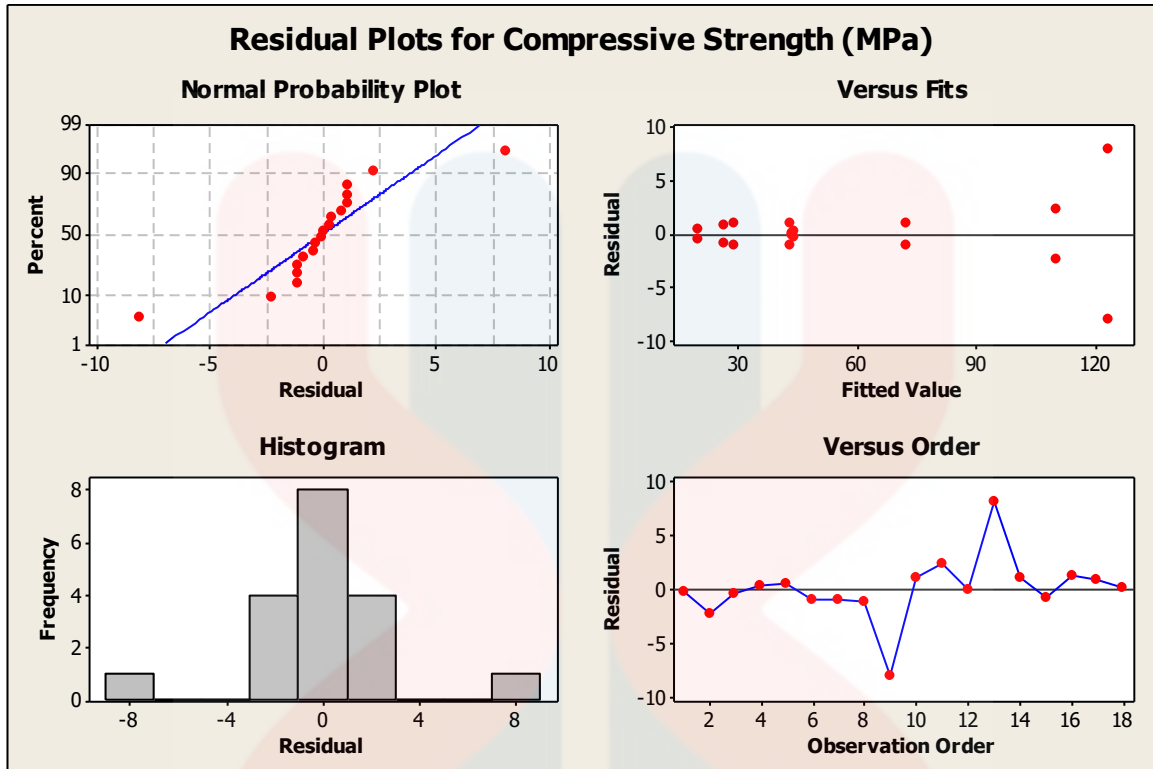


Figure 4.4 (e): Residual plots for compressive strength; (i) Normal probability plot, (ii) Histogram of frequency versus residual, (iii) Residual versus fits, (iv) Residual versus observation order of data

An examination of all normal probability plots reveals that the majority of the residual points, with the exception of bulk density, are dispersed about the straight line. This proved that the data for linear shrinkage, water absorption, apparent porosity, and compressive strength are normal distributed, and it also indicated that the first criteria of model appropriateness testing was fulfilled. In addition, the histogram plot showed that the histogram bar was almost perfectly symmetrical, with the exception of linear shrinkage and water absorption. As a result, the facts in issue offer support to the usual distribution of linear shrinkage, water absorption, apparent porosity, bulk density and compressive strength.

From that point on, all histogram of linear shrinkage, water absorption, apparent porosity, bulk density, and compressive strength had the same pattern as the standard histogram. For linear shrinkage, water absorption, apparent porosity, bulk density, and compressive strength, this offers the typical distribution statistics that are often used. The pattern was created in the shape of a dumbbell, which suggests that any data is periodically distributed in a manner that is consistent. The data for water absorption, apparent porosity, bulk density, and compressive strength were found to be randomly distributed, which satisfies the criteria of constant residual variance. This was discovered by the plotting of residuals against modified values. Given that the residual is evaluated in relation to the order of observations, it can be shown that the points that constitute the residual are entirely unaffected by the order of observations. The residuals were thought to be independent of one another, as stated in the previous assumption.

4.2.3 Analysis of Variance (ANNOVA)

In the great majority of statistical experimental studies, the research methodology known as analysis of variance (ANOVA) was used. The purpose of this technique was to determine whether or not a certain operational component had significant effects on the properties or reactions of a particular application or product that was developed. In order to discover the weight % of WS and the sintering temperature that had a significant impact on linear shrinkage, water absorption, apparent porosity, bulk density, and compressive strength, an analysis of variance (ANOVA) was performed. This was achieved by observing on the probability value, which is often commonly referred to as the "p-value," over the course of the research.

Evaluation of the data that was obtained was carried out with the assistance of the statistical software known as MINITAB 16. The p-value is used in order to investigate the statistical significance of the model. In point of fact, such an examination is carried out. When conducting an analysis of the statistical hypothesis, the p-value, which is also referred to as the probability value, for a particular statistical model indicates the likelihood, that the statistical summary will be greater than the actual findings observed or equal to them (for example, the absolute mean difference between the two comparative classes of the sample). The p-value between should be less than 0.05 as a result of this decision. Following that, it was shown that the quadratic model takes into account the components that are statistically important.

Table 4.2 (a): ANOVA for linear shrinkage of porous ceramic added with WS

Source	P-value
Wt.% WS	0.00
Sintering Temperature	0.00
Wt.% WS*Sintering Temperature	0.00

Table 4.2 (b): ANOVA for water absorption of porous ceramic added with WS

Source	P-value
Wt.% WS	0.00
Sintering Temperature	0.00
Wt.% WS*Sintering Temperature	0.00

Table 4.2 (c): ANOVA for apparent porosity of porous ceramic added with WS

Source	P-value
Wt.% WS	0.00
Sintering Temperature	0.00
Wt.% WS*Sintering Temperature	0.00

Table 4.2 (d): ANOVA for bulk density of porous ceramic added with WS

Source	P-value
Wt.% WS	0.00
Sintering Temperature	0.357
Wt.% WS*Sintering Temperature	0.517

Table 4.2 (e): ANOVA for compressive strength of porous ceramic added with WS

Source	P-value
Wt.% WS	0.00
Sintering Temperature	0.00
Wt.% WS*Sintering Temperature	0.00

The results of the analysis of variance (ANOVA) linear shrinkage, water absorption, apparent porosity, bulk density, and compressive strength of porous ceramics incorporated with WS are shown in Tables 4.2 (a) to 4.2 (e). Based on the findings, it was discovered that the p-value for the linear factor of wt.% of WS for linear shrinkage, water absorption, apparent porosity, bulk density, and compressive strength is zero (0.000), respectively. It is statistically significant, as shown by the p-value, which is less than 0.05. According to literature, a lower p-value suggests that there is a stronger relationship among two variables. This demonstrates that the different wt.% of WS that is added has an effect on water absorption, apparent porosity, bulk density, and compressive strength.

Besides that, the p-value for the linear factor of sintering temperature and the wt.% WS*sintering temperature interaction factor for other responses, such as linear shrinkage, water absorption, apparent porosity, bulk density, and compressive strength, is less than 0.05. This is applicable for all responses. Both the linear factor of the sintering temperature and the interaction factor of the wt.% of WS multiplied by the sintering temperature did not have a substantial impact on any of the solutions, as shown by the fact that their p-values were quite low. Specifically, this is because of the temperature at which the sintering process takes place. As the temperature increases, the clay particles start to combine with one another, and as the temperature keeps increasing, they dissolve and fill the spaces between the pores that are generated by the sintering process. Not only did the higher temperatures cause the WS to be burnt, but they also caused the clay particles to meld together, which ultimately led to the pores of the porous ceramic being closed up more completely. Therefore, it is possible to draw the conclusion that the sintering temperature does not have a more substantial effect; rather, the role of the various wt.% of WS that is added has only a considerable influence on the reaction, which includes linear shrinkage, water absorption, apparent porosity, bulk density, and compressive strength.

4.2.4 Main Effects and Interaction Plots

The main effects plot shows the influence of a factor (at a number of different levels) on the variations in a particular response. In this typical factorial design, the most important factors that were evaluated were the weight percentage of WS and the temperature at which the sintering process was carried out. The interaction plot, on the other hand, illustrates the combined impact of the two principal components of the particular response (at different levels) (linear shrinkage, water absorption, apparent porosity, bulk density, or compressive strength of the material). Figure 4.5 (a) to Figure 4.5 (e) has shown the main effect plot of linear shrinkage, water absorption, apparent porosity, bulk density, and compressive strength. In meanwhile Figure 4.6 (a) to Figure 4.6 (e) shows interaction plot for linear shrinkage, water absorption, apparent porosity, bulk density, and compressive strength respectively.

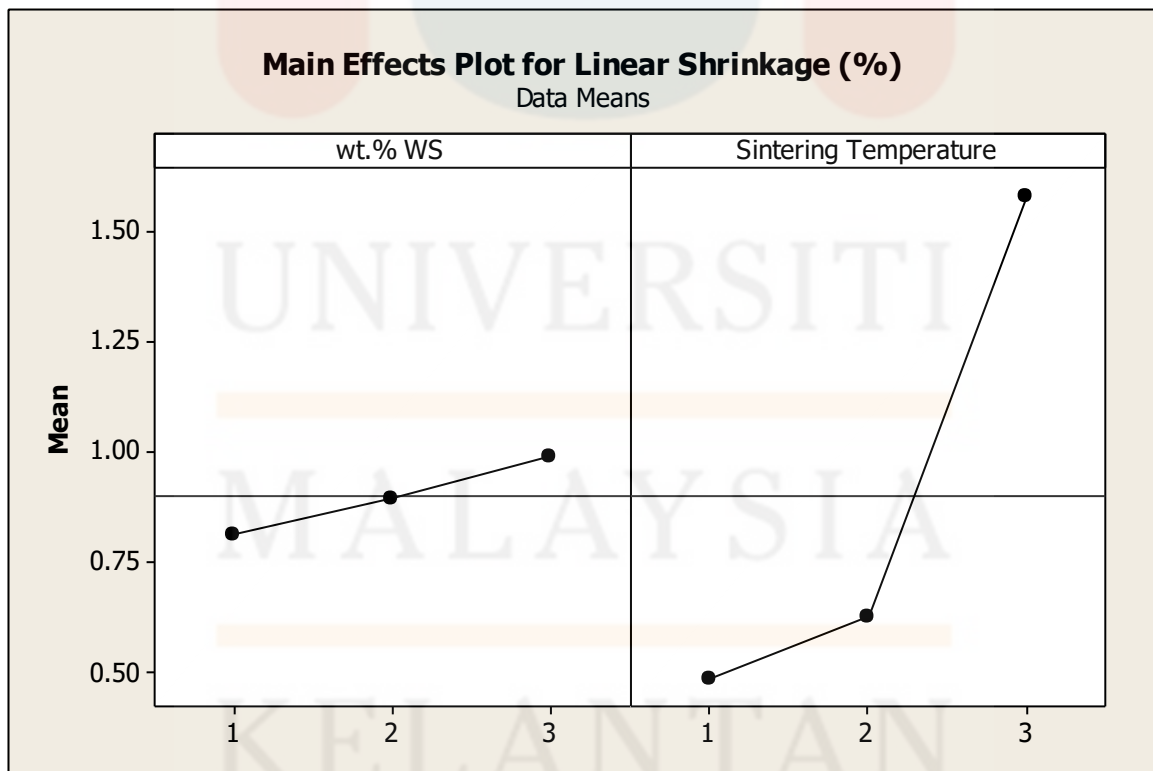


Figure 4.5 (a): Main effects plots for linear shrinkage

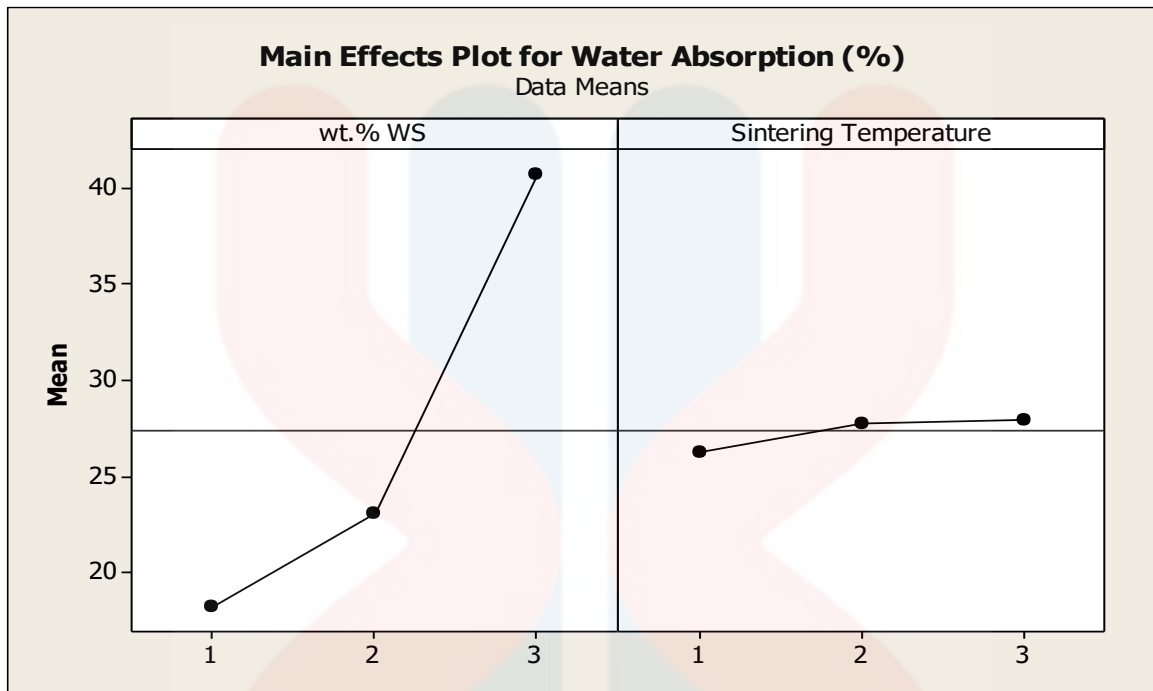


Figure 4.5 (b): Main effects plots for water absorption

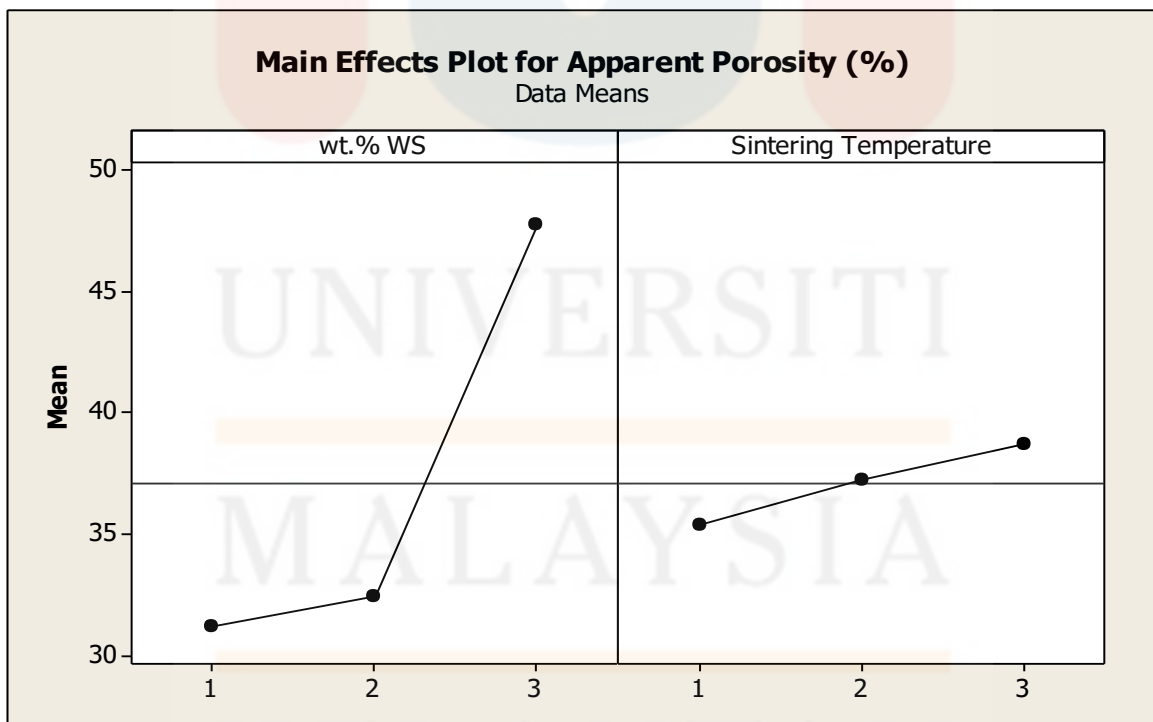


Figure 4.5 (c): Main effects plots for apparent porosity

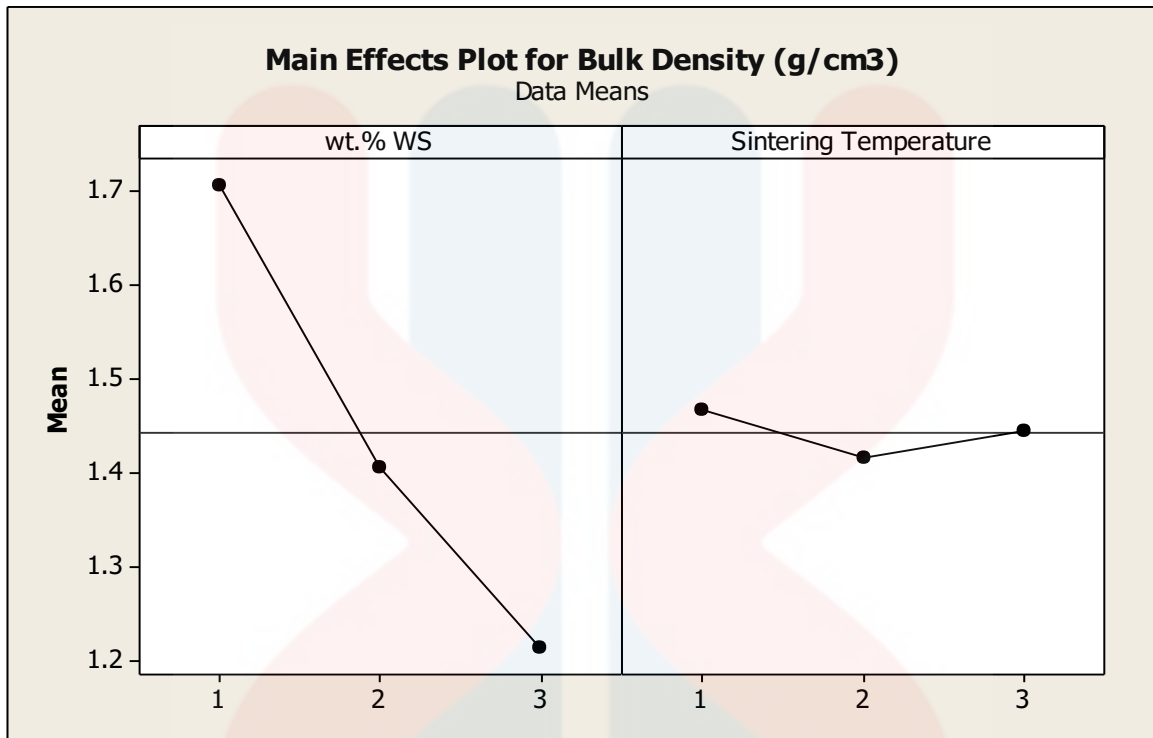


Figure 4.5 (d): Main effects plots for bulk density

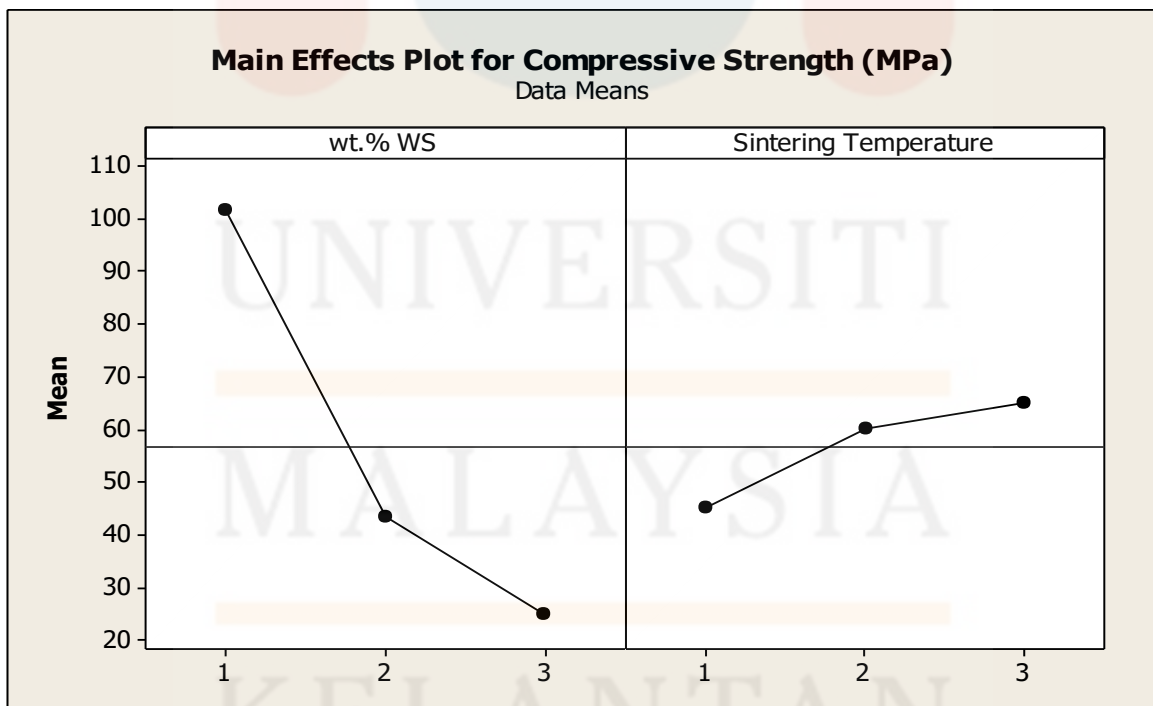


Figure 4.5 (e): Main effects plots for compressive strength

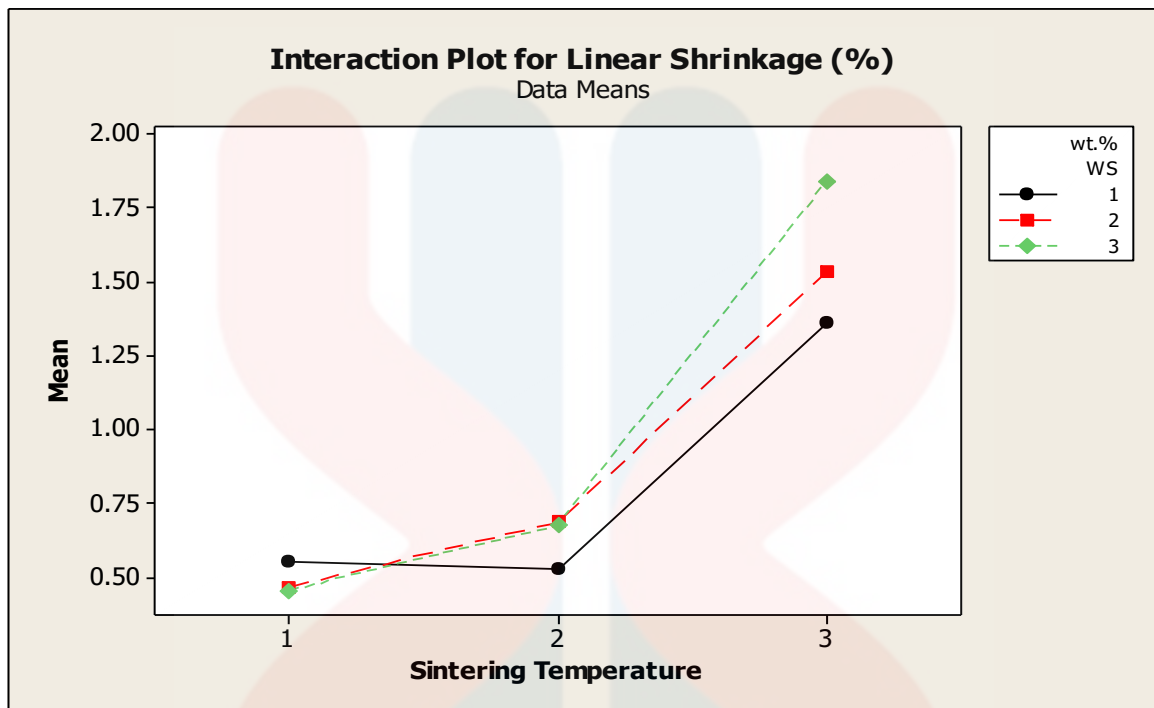


Figure 4.6 (a): Interaction plots for linear shrinkage

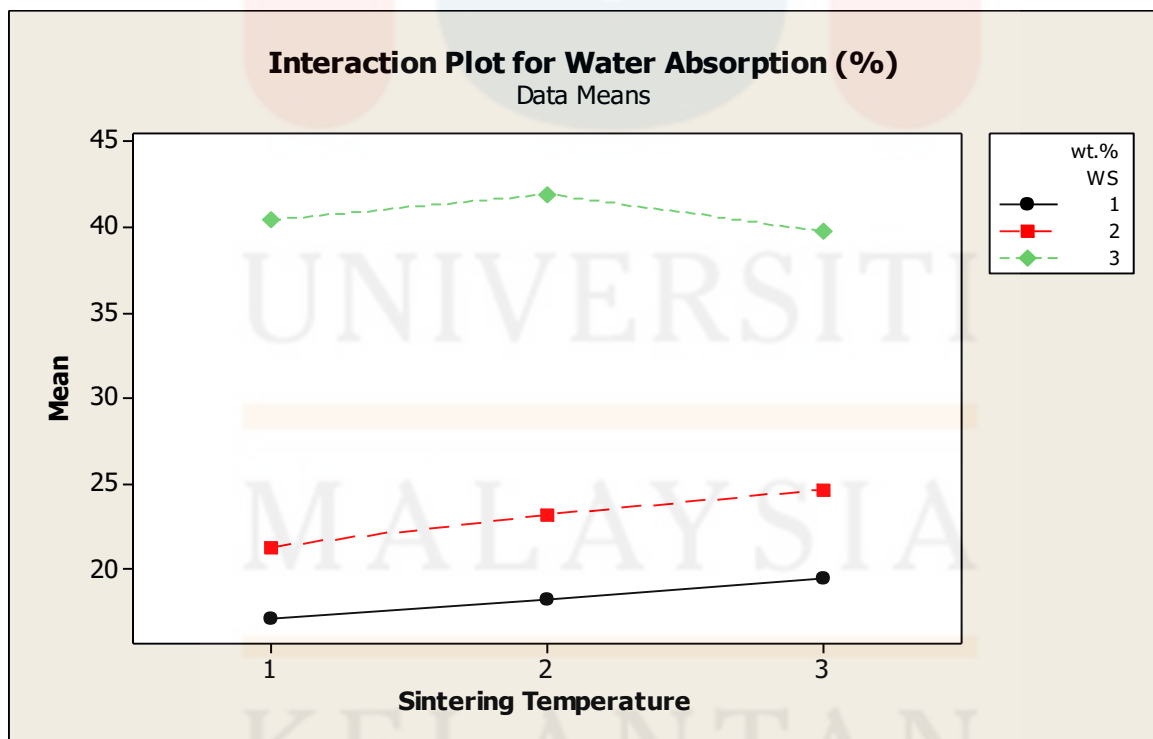


Figure 4.6 (b): Interaction plots for water absorption

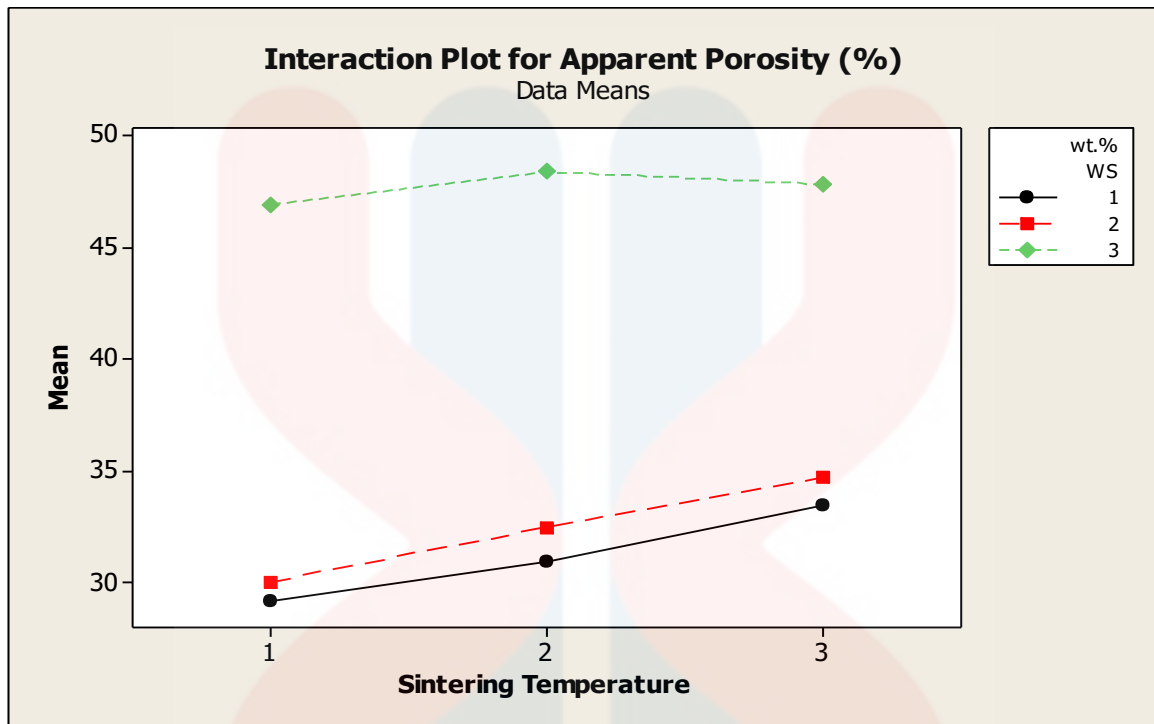


Figure 4.6 (c): Interaction plots for apparent porosity

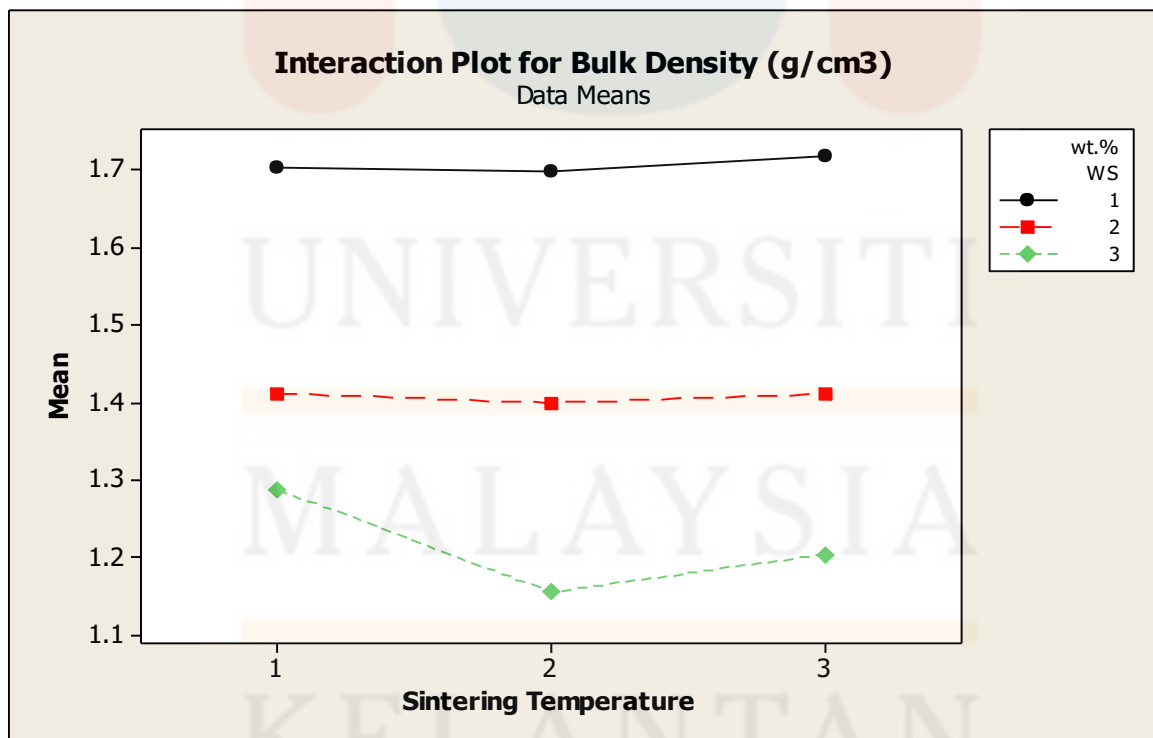


Figure 4.6 (d): Interaction plots for bulk density

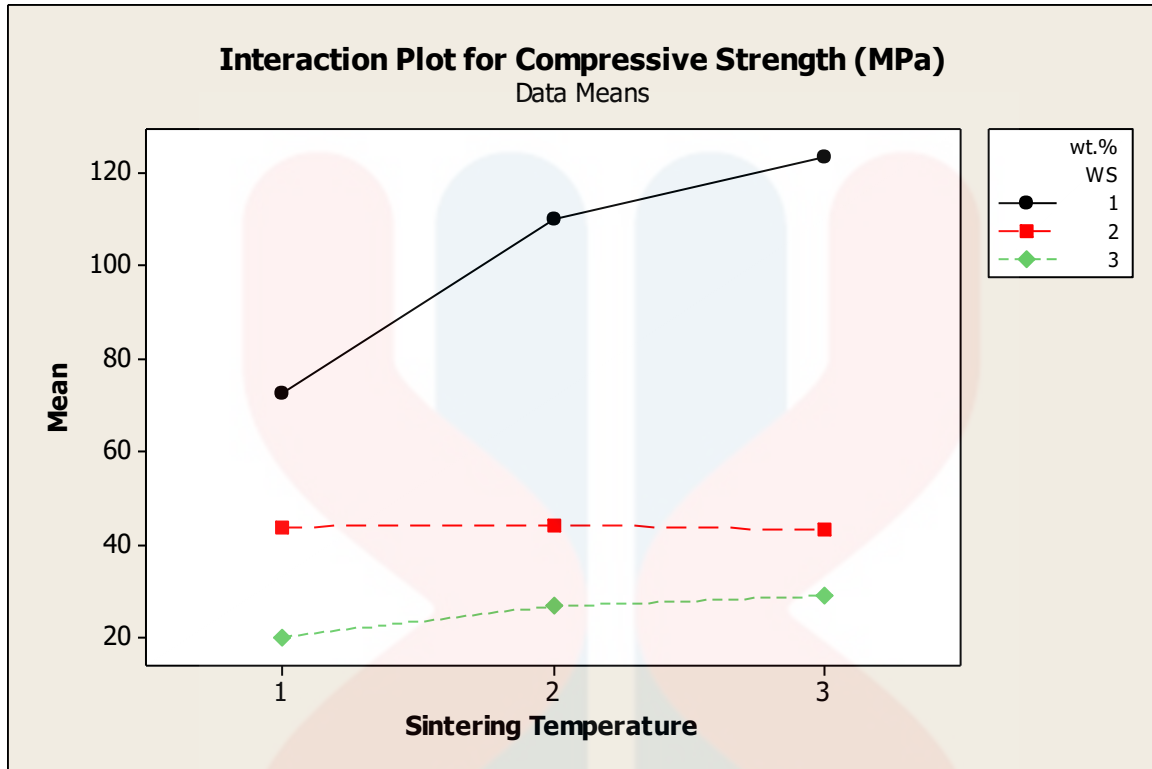


Figure 4.6 (e): Interaction plots for compressive strength

Figure 4.5 (a), which shows the main effects plots for linear shrinkage, indicates that an increase in the weight percentage of walnut shell added from 0 wt.% (coded as '1') to 20 wt.% (coded as '3') leads to a higher linear shrinkage for the porous ceramic. This is shown by the fact that the linear shrinkage is increased. Aside from that, the sintering temperature for linear shrinkage is exhibiting a tendency of increasing from 850°C (coded as '1') to 950°C (coded as '3'). In the meanwhile, Figure 4.6 (a) shows the line that represents the interaction plot. This line is not parallel, which indicates that there is a huge interaction between the factors (particularly the wt.% of walnut shell and the sintering temperature). During thorough analysis, it was determined that the porous ceramic that included 30 wt.% of walnut shell showed the highest linear shrinkage. Increasing the temperature at which the sintering process is carried out causes the sintered compact to get denser. This is because the pores are absorbed in the ceramic phase via particulate wetting, which causes the product to become densifies, as seen by the linear shrinkage (Love, 2017).

The main effects plots for water absorption are shown in Figure 4.5 (b), and they show that an increase in the weight percentage of walnut shell applied from 0 wt.% (coded as '1') to 20 wt.% (coded as '3') brings about an increase in the amount of water that is absorbed by the porous ceramic. In addition to this, the sintering temperature for water absorption shows a pattern of increasing progressively from 850°C (coded as '1') to 950°C (coded as '3'). On top of that, Figure 4.6 (b) shows the line that represents the interaction plot. This line indicates that there is a significant interaction between the following factors: the wt.% of walnut shell and the sintering temperature. Base on that, it turned out that the porous ceramic that included 30 wt.% of walnut shell showed the best water absorption. This is due to the fact that consisting of a PFA into the ceramic will result in an increase in the porosity of the material as well as an increase in its capacity to water absorption (Beal et al., 2019).

As shown in Figure 4.5 (c), the main effect plot of the apparent porosity is shown. As a result of the analysis of the main effect plot, it indicates a pattern to increase as the wt.% of walnut shell that is added increases. This is due to the fact that the number of voids, also known as pores, in porous ceramic increases as the wt.% of walnut shell is increased. Following that, the influence on apparent porosity for sintering temperature shows a trend of increasing from 850 °C (where '1' is coded) to 950 °C (where '3' is coded). A high interaction between the two factors (wt.% walnut shell and sintering temperature) is given by the fact that the lines in the interaction plot are not parallel, as shown in Figure 4.6 (c). This indicates that the interaction could be significant. Following a thorough analysis, it was determined that the porous ceramic that included 30 wt.% of walnut shell had the highest apparent porosity. After that, the further analysis for the plot shown that the apparent porosity of the porous ceramic decreased with increasing sintering temperature, regardless of the wt.% of walnut shell that was added to the mixture. The porous ceramic that had 30 wt.% of walnut shell added to it, along with the sintering period of 900°C, showed the highest apparent

porosity. The effect of sintering temperature on porous ceramic likewise shows a decreasing pattern, in which the increasing length of the sintering time results in a decrease in the apparent porosity of the porous ceramic.

It turned out in Figure 4.5 (d), based on the main effects plot, that increasing the weight of walnut shell added from 0 wt.% (coded as '1') to 30 wt.% (coded as '3') results in a falling trend caused by the fact that the quantity of walnut shell added is increasing. The main effect plots indicate a decrease in the trend for the sintering temperature in bulk density, beginning at 850°C (coded as '1') and until at 900°C (coded as '2'). On the other hand, the trend begins to increase in 950°C (coded as '3'). According to Figure 4.6 (d), the interaction plot of the bulk density, the highest result is shown at the 0 wt.% (coded as '1') of walnut shell that is combined with a combination of 950°C (coded as '3') of sintering temperature and walnut shell. This shows that the addition of walnut shell into porous ceramic as a PFA will result in a decrease in the overall density of the material. In the meanwhile, the line is parallel to one another, as shown by the observation. This indicates that there is no connection between the reaction and both the temperature or the weight (A & Kulami. 2017).

The main effects plots for compressive strength are shown in Figure 4.5 (e), which shows that an increase in the wt.% of walnut shell added from 0 wt.% (coded as '1') to 30 wt.% (coded as '3') results in a decreasing trend. This is due to the fact that the amount of walnut shell added is rising. According to the interaction plot of the compressive strength, which can be seen in Figure 4.6 (e), the highest value appears at the 0 wt.% (coded as '1') of walnut shell that is coupled with a combination of 950 °C (coded as '3') of sintering temperature and walnut shell. The fact that this is the case indicates that the incorporation of walnut shell into porous ceramic as a PFA will lead to a reduction in the total strength produced by the material. Pores in ceramic structures will lead to stress increase during compressive testing, which will result in a decrease in the strength of ceramic materials. As

the number of pores in the membrane increases, the membrane becomes brittle and is more likely to crack or rupture when tested to a strength test (Rahim et al., 2019).

4.2.5 Contour plot and its application

The contour plot is a graphical illustration of the regression model that shows the responses (linear shrinkage, water absorption, apparent porosity, bulk density, and compressive strength) in connection with the that desired factors (wt.% of WS and sintering temperature). Figure 4.x to Figure 4.x shows the contour plots for linear shrinkage, water absorption, apparent porosity, bulk density, and compressive strength. These plots may be found in relation to each other. Following closer observation, it was possible to see that all of the contour plot was built up of contour or curve lines. The presence of an interaction between the wt.% of WS (factor A) and the firing temperature (factor B) is further supported by this further evidence.

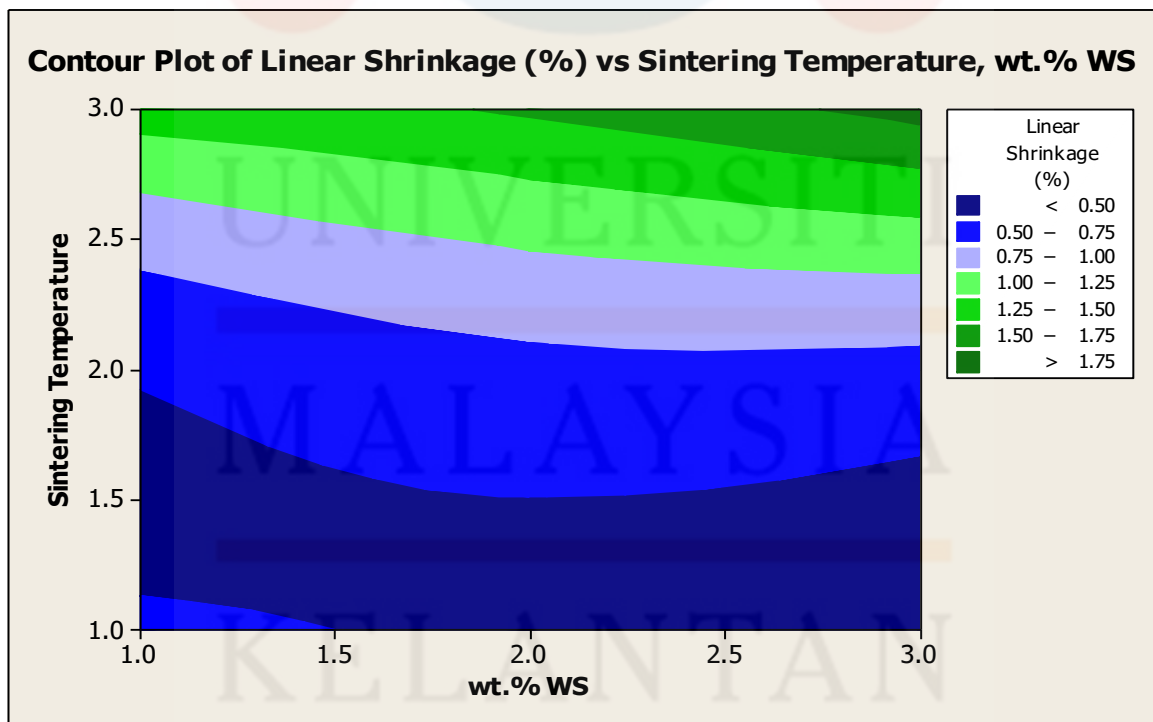


Figure 4.7 (a): Contour plot of linear shrinkage (%) vs sintering temperature, wt.% WS.

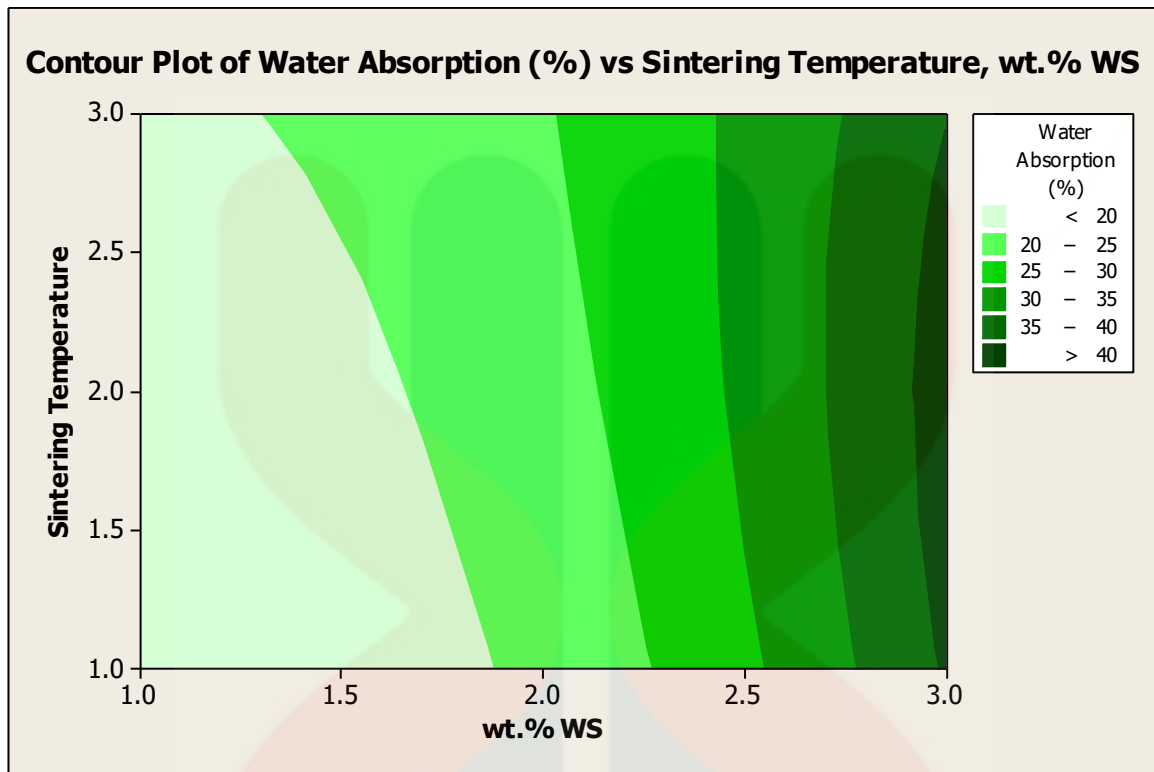


Figure 4.7 (b): Contour plot of water absorption (%) vs sintering temperature, wt.% WS.

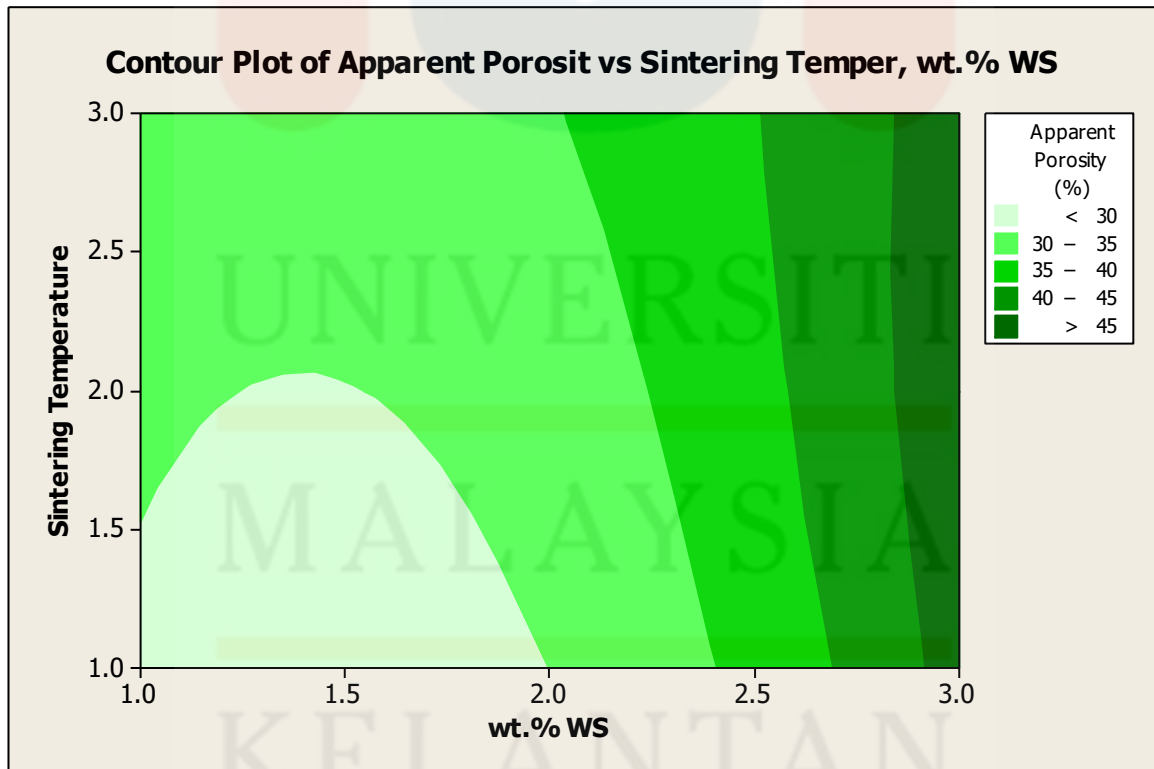


Figure 4.7 (c): Contour plot of apparent porosity (%) vs sintering temperature, wt.% WS.

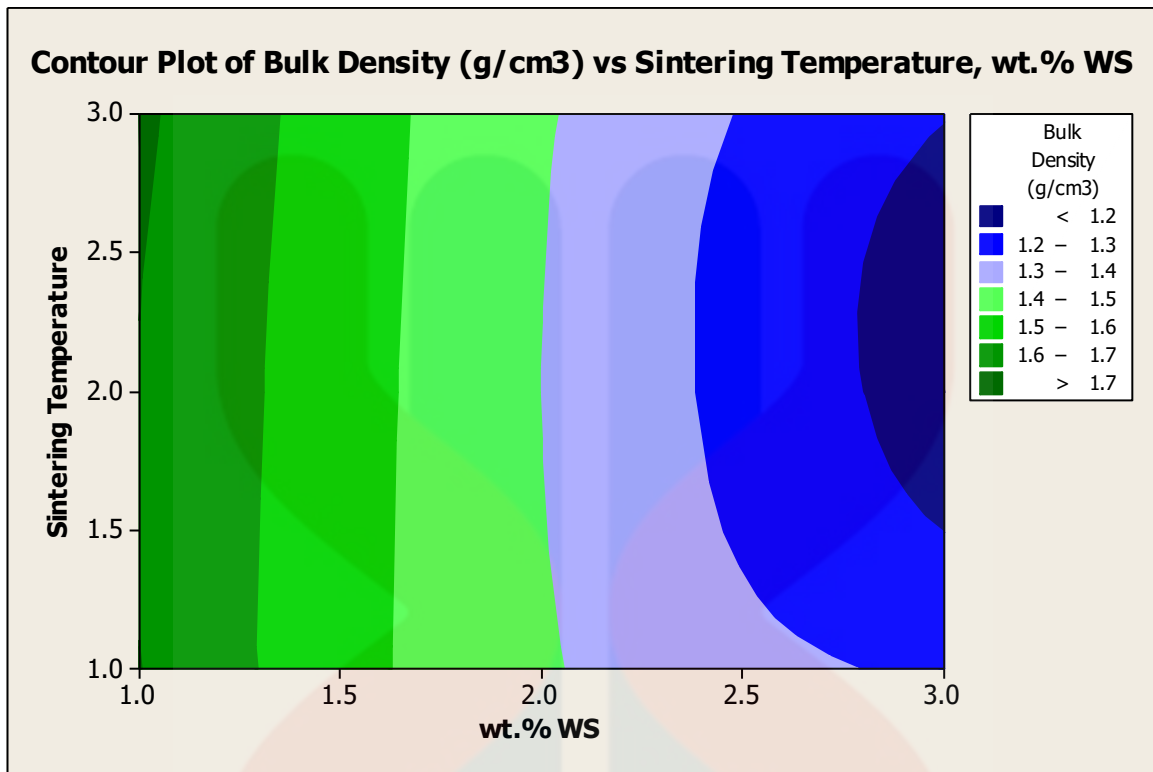


Figure 4.7 (d): Contour plot of bulk density (g/cm³) vs sintering temperature, wt.% WS.

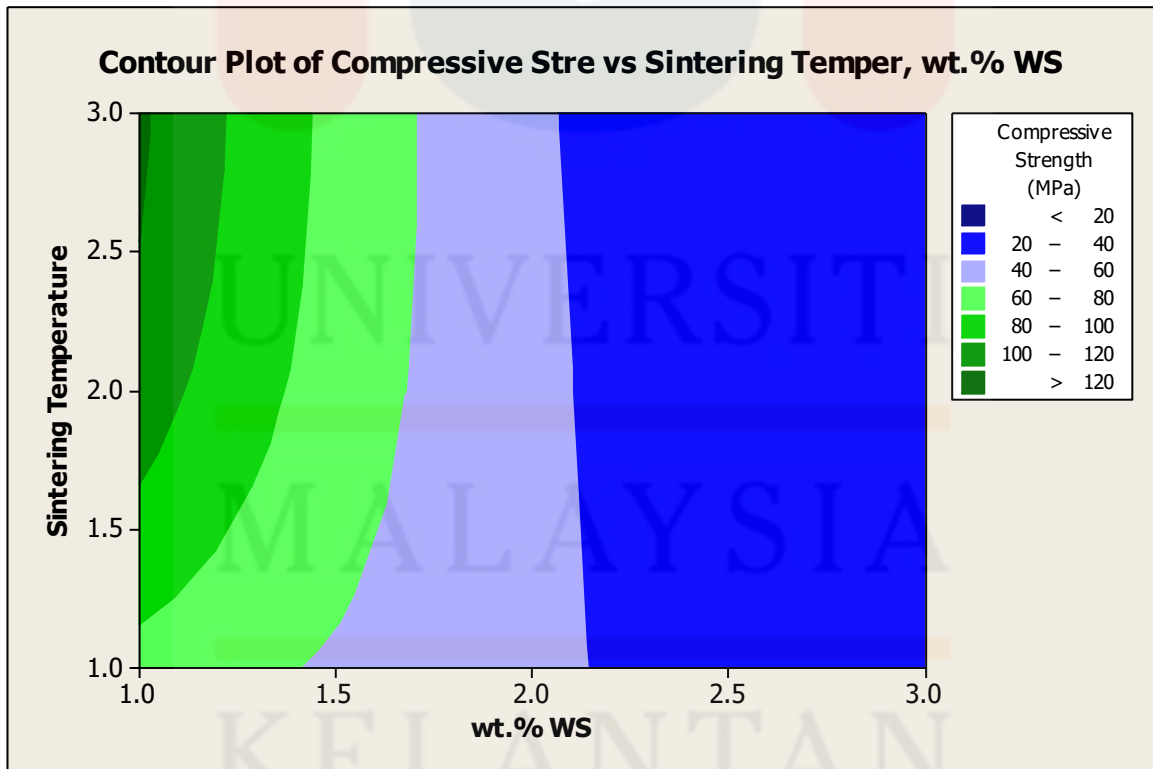


Figure 4.7 (e): Contour plot of compressive strength (MPa) vs sintering temperature, wt.% WS.

4.3 XRD Analysis Incorporated with Walnut Shell

This investigation consisted of porous ceramic samples with a weight percentage of 10 wt.% of WS (sintering temperature 850 and 950° C) and porous ceramics with a weight percentage of 20 wt.% of WS (sintering temperature 950° C). The selection was made with the intention of determining the crystalline phase of porous ceramic by using a variety of weight percentages of WS combined with a number of different sintering temperatures. Porous ceramics are characterised by X-ray diffraction, as shown in Figure 4.8 (a) to Figure 4.8 (c) and Figure 4.9.

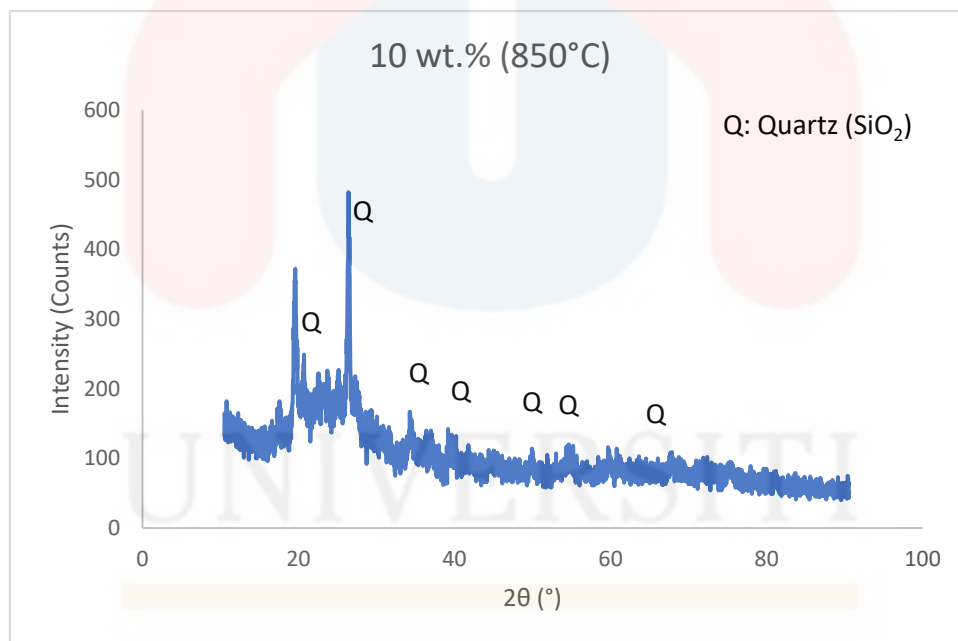


Figure 4.8 (a): XRD characterization of the porous ceramic 10 wt.% (850°C)

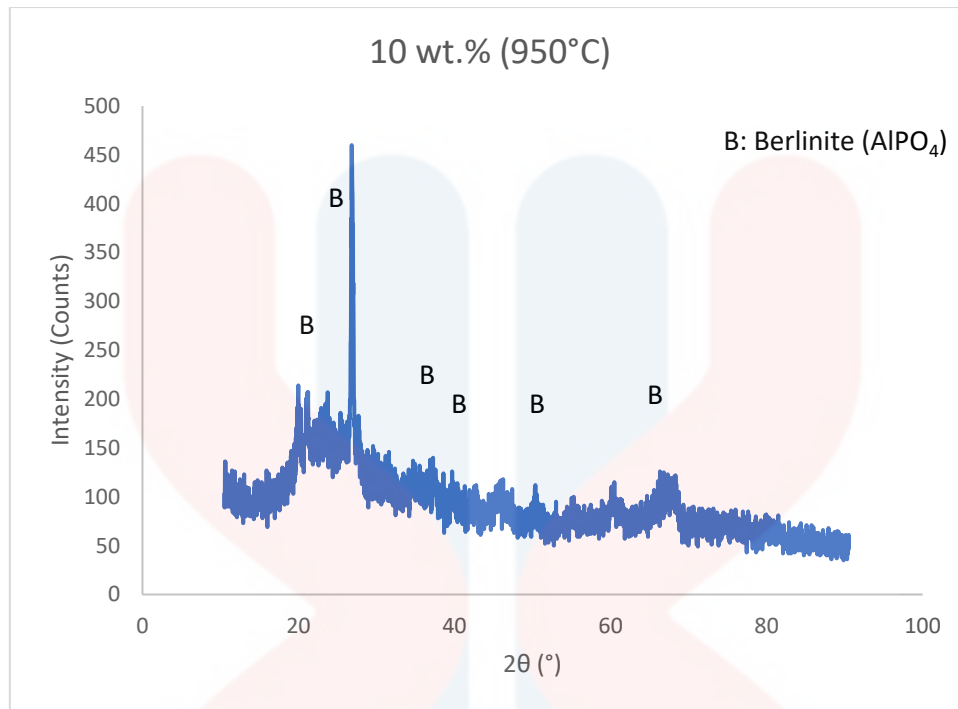


Figure 4.8 (b): XRD characterization of the porous ceramic 10 wt.% (950°C)

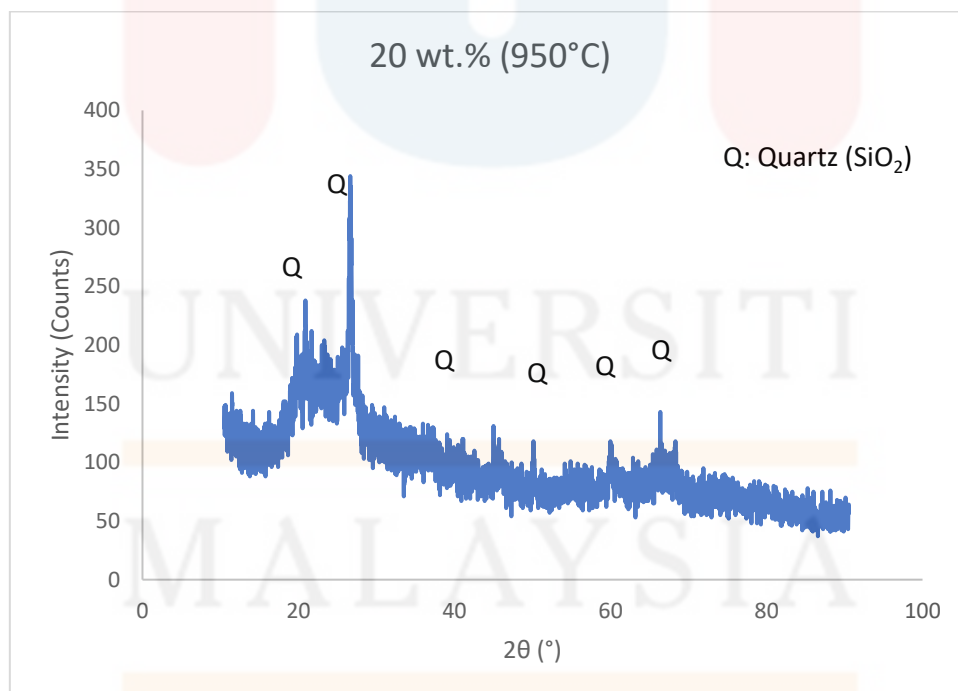


Figure 4.8 (c): XRD characterization of the porous ceramic 20 wt.% (950°C)

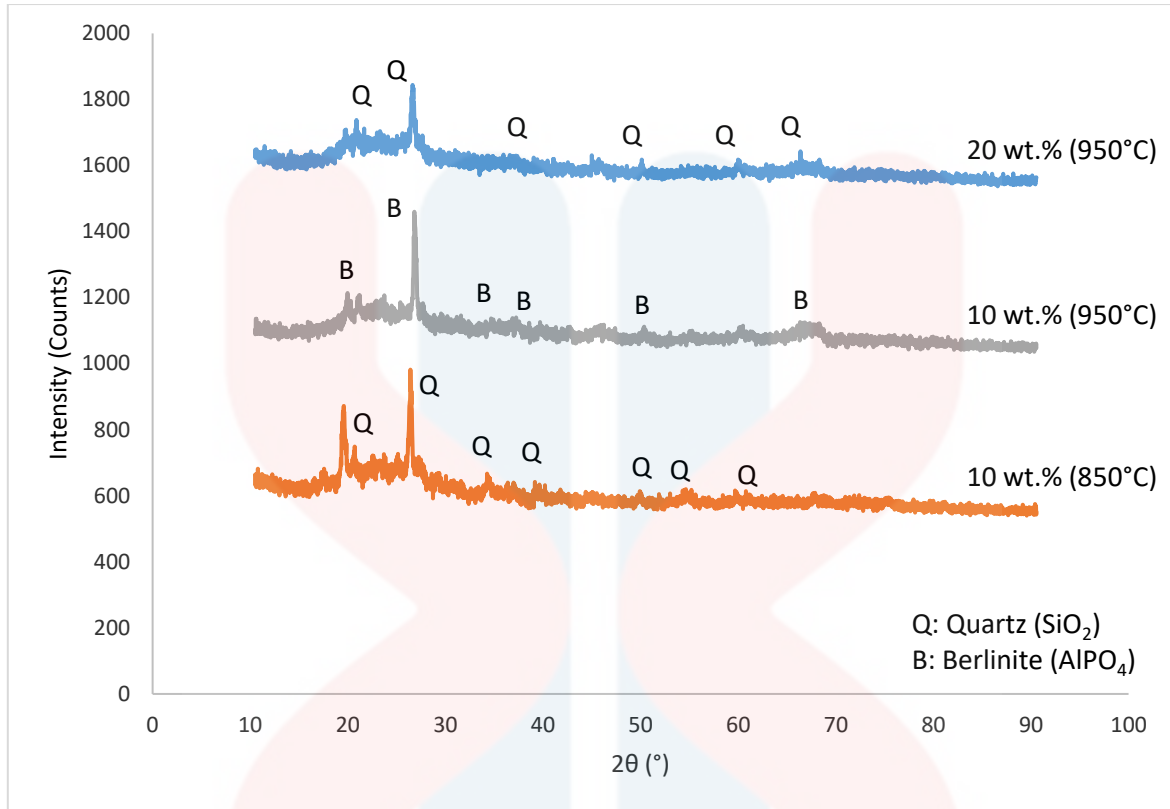


Figure 4.9: XRD characterization of the porous ceramic

Based on Figure 4.8 (a) and Figure 4.8 (c), crystalline phases were observed in the porous ceramic incorporated with 10 wt.% of WS at 850°C sintering temperature and 20 wt.% of WS at 950°C sintering temperature: quartz (COD9010144). The phase starts changing when the weight percentage of WS increases and stops changing when increasing the sintering temperature. The phases in the sample starting disappear at high temperatures and completely change at higher temperatures (Anuar et al., 2020). This has proven why compressive strength at 10 wt.% of WS at 850°C sintering temperature has higher compressive strength, and 20 wt.% of WS at 950°C sintering temperature has slightly lower compressive strength. The increased compressive strength of the porous ceramic is a result of its decreased porosity. This has proven the bulk density of the porous ceramic incorporated with 10 wt.% of WS at 850°C sintering temperature is higher than 20 wt.% of WS at 950°C

sintering temperature. Higher densification results in more closure of the pores, increasing the bulk density. Lower porosity will result from more closed pores.

Moreover, according to Figure 4.8 (b), the distinct crystalline phases were observed in the porous ceramic incorporated with 10 wt.% of WS at 950°C sintering temperature, which is berlinite (COD9006549). Berlinite, with the chemical formula AlPO_4 , is a rare high-temperature hydrothermal or metasomatic phosphate mineral. It shares the same crystal structure as quartz (Warr, 2021). The compressive strength value for 10 wt.% of WS is 43.67 MPa higher than 20 wt.% of WS which is 29.9 MPa. The compressive strength is related to the hardness of the crystalline phase on the porous ceramic. Every crystalline phase present in the porous ceramic has its own hardness value can be clarified by the Mohs hardness scale. Mohs hardness scale correspondents to the compressive strength (Top & Vapur, 2018). Table 4.2 shows the Mohs hardness scale of the crystalline phase in porous ceramic incorporated with walnut shell.

Table 4.3: Mohs hardness scale of the crystalline phase.

Crystalline Phase	Mohs Hardness Scale	References
Quartz	7	(Z. Li et al., 2019)
Berlinite	6.5	(Warr, 2021)

From what can be shown in Table 4.2, every single crystalline phase has an outstanding Mohs hardness scale. This has shown that even the 10 wt.% of WS has a high porosity in porous ceramic. The Mohs hardness of crystalline phase that is present in 10 wt.% of WS helps to increase the compressive strength in this composition.

CHAPTER 5

CONCLUSION AND RECOMMENDATIONS

5.1 Conclusion

The results of the research project showed the immense potential for incorporating walnut shell as a (PFA) in the production of porous ceramics. It is possible to draw the following conclusion on the basis of the findings that were provided and analyzed in Chapter 4:

- a) The use of walnut shell as a pore-forming agent (PFA) for porous ceramic products has been determined to be acceptable using walnut shell. In addition, it was discovered that the percentage of weight and the temperature at which the sintering process took place had a considerable impact on the physical and mechanical properties of porous ceramic.
- b) At the sintering temperature of 950°C, the porous ceramic that is combined with walnut shell has a strength that from 10 wt.% of WS to 20 wt.% of WS. The lowest strength of this material is achieved at the same temperature. When it comes to apparent porosity, the greatest value is 20 wt.% of WS when the sintering temperature is 900°C, and the lowest value is 10 wt.% of WS when the sintering temperature is 850°C. As a result, the porous ceramic that was included with 10 wt.% of WS and a sintering temperature of 950°C was able to achieve a composition and sintering characteristics that were optimally matched.

5.2 Recommendations

The porous ceramic should be analyzed further using scanning electron microscopy (SEM) to examine its morphology once the sintering temperature has been reached, particularly the distribution of porosity and the size of pores. Increasing the compressive strength of porous ceramic by incorporating silica (a filler) or feldspar (a flux) into the body composition during the manufacturing process.

REFERENCES

- Akhmadiyeva, N., Abdulvailyev, R., Abikak, Y., Manapova, A., Gladyshev, S., Ruzakhunova, G., & Sukurov, B. (2023). Kaolinite clay as a raw material for erbium extraction. *Heliyon*, 9(4).
- Albatrni, H., Qiblawey, H., & Al-Marri, M. J. (2022). Walnut Shell based adsorbents: A review study on preparation, mechanism, and application. *Journal of Water Process Engineering*, 45, 102527. <https://doi.org/10.1016/j.jwpe.2021.102527>
- ALI, M. S., HANIM, M. A., TAHIR, S. M., JAAFAR, C. N., NORKHAIRUNNISA, M., & MATORI, K. A. (2017). Preparation and characterization of porous alumina ceramics using different pore agents. *Journal of the Ceramic Society of Japan*, 125(5), 402–412. <https://doi.org/10.2109/jcersj2.16233>
- Auvert, G. (2017). Difference in Number of Electrons in Inner Shells of Charged or Uncharged Elements in Organic and Inorganic Chemistry: Compatibility with the Even-Odd Rule. *Open Journal of Physical Chemistry*, 07(02), 72–88. <https://doi.org/10.4236/ojpc.2017.72006>
- Beskopylny, A., Stel'makh, S., Shcherban', E., Mailyan, L., Meskhi, B., Shilov, A., Chernil'nik, A., & El'shaeva, D. (2023). Effect of walnut-shell additive on the structure and characteristics of concrete. *Materials*, 16(4), 1752. <https://doi.org/10.3390/ma16041752>

- Chakraborty, S., Uppaluri, R., & Das, C. (2020). Effect of pore former (saw dust) characteristics on the properties of sub-micron range low-cost ceramic membranes. *International Journal of Ceramic Engineering & Science*, 2(5), 243–253. <https://doi.org/10.1002/ces2.10061>
- Chen, Y., Wang, N., Ola, O., Xia, Y., & Zhu, Y. (2021). Porous ceramics: Light in weight but heavy in energy and Environment Technologies. *Materials Science and Engineering: R: Reports*, 143, 100589. <https://doi.org/10.1016/j.msar.2020.100589>
- Dele-Afolabi, T. T., Azmah Hanim, M. A., Jung, D. W., Ilyas, R. A., Calin, R., & Nurul Izzah, A. R. (2022). Rice husk as a pore-forming agent: Impact of particle size on the porosity and diametral tensile strength of porous alumina ceramics. *Coatings*, 12(9), 1259. <https://doi.org/10.3390/coatings12091259>
- Dele-Afolabi, T. T., Hanim, M. A. A., Norkhairunnisa, M., Sobri, S., & Calin, R. (2017). Research trend in the development of macroporous ceramic components by pore forming additives from Natural Organic Matters: A short review. *Ceramics International*, 43(2), 1633–1649. <https://doi.org/10.1016/j.ceramint.2016.10.177>
- Eva, G., Zuzana, Z., & Willi, P. (2008). Porous Ceramic Made Using Potato Starch as a Pore-forming Agent. *Fruit, Vegetable and Cereal Science and Biotechnology*, 3(Special Issue 1).
- German, R. M., Suri, P., & Park, S. J. (2009). Review: Liquid phase sintering. *Journal of Materials Science*, 44(1), 1–39. <https://doi.org/10.1007/s10853-008-3008-0>

- Goel, G., & Kalamdhad, A. S. (2017). An investigation on use of paper mill sludge in brick manufacturing. *Construction and Building Materials*, 148, 334–343.
<https://doi.org/10.1016/j.conbuildmat.2017.05.087>
- Hossain, S. S., & Roy, P. K. (2020, October 1). *Sustainable ceramics derived from solid wastes: A review – doaj*. Journal of Asian Ceramic Societies.
<https://doaj.org/article/4d654380b01a44c18251e52f7e91e1e0>
- Hübner, C., Vadalà, M., Voges, K., & Lupascu, D. C. (2023). Poly(vinyl alcohol) freeze casts with nano-additives as potential thermal insulators. *Scientific Reports*, 13(1).
<https://doi.org/10.1038/s41598-022-27324-2>
- Kumar, H., Bhardwaj, K., Sharma, R., Nepovimova, E., Kuča, K., Dhanjal, D. S., Verma, R., Bhardwaj, P., Sharma, S., & Kumar, D. (2020, June 18). *Fruit and vegetable peels: Utilization of high value horticultural waste in novel industrial applications*. MDPI.
<https://doi.org/10.3390%2Fmolecules25122812>
- Kwon, Y.-M., Chang, I., & Cho, G.-C. (2023). Consolidation and swelling behavior of kaolinite clay containing xanthan gum biopolymer. *Acta Geotechnica*.
<https://doi.org/10.1007/s11440-023-01794-8>
- Liu, T., Tang, Y., Han, L., Song, J., Luo, Z., & Lu, A. (2017). Recycling of harmful waste lead-zinc mine tailings and fly ash for preparation of inorganic porous ceramics. *Ceramics International*, 43(6), 4910–4918.
<https://doi.org/10.1016/j.ceramint.2016.12.142>
- Love, B. J. (2017). Ceramic Biomaterials. In *Elsevier eBooks* (pp. 185–204).
<https://doi.org/10.1016/b978-0-12-809478-5.00008-0>

- Mouiya, M., Bouazizi, A., Abourriche, A., Khessaimi, Y. E., Benhammou, A., Hafiane, Y. E., Taha, Y., Oumam, M., Abouliatim, Y., Smith, A., & Hannache, H. (2019). Effect of sintering temperature on the microstructure and mechanical behavior of porous ceramics made from clay and banana peel powder. *Results in Materials*, 4, 100028. <https://doi.org/10.1016/j.rinma.2019.100028>
- Pia, G., Casnedi, L., & Sanna, U. (2015). Porous ceramic materials by pore-forming agent method: An intermingled fractal units analysis and procedure to predict thermal conductivity. *Ceramics International*, 41(5), 6350–6357. <https://doi.org/10.1016/j.ceramint.2015.01.069>
- Rahim, F. a. M., Noh, M. Z., Rashid, M. W. A., Mohamed, J. J., & Nor, M. a. a. M. (2019). Preparation and characterization of ceramic membrane by using palm fibers as pore forming agent. *AIP Conference Proceedings* 2068, 020056 (2019). <https://doi.org/10.1063/1.5089355>
- Saeed Salih, H. (2020). Physicochemical properties of walnuts (*Juglans regia* L.) shells and kernels growing in different locations in Kurdistan Region-iraq. *Journal of Zankoy Sulaimani - Part A*, 22(2), 109–118. <https://doi.org/10.17656/jzs.10812>
- Salleh, S. Z., Awang Kechik, A., Yusoff, A. H., Taib, M. A., Mohamad Nor, M., Mohamad, M., Tan, T. G., Ali, A., Masri, M. N., Mohamed, J. J., Zakaria, S. K., Boon, J. G., Budiman, F., & Teo, P. T. (2021). Recycling Food, agricultural, and industrial wastes as pore-forming agents for sustainable porous ceramic production: A Review. *Journal of Cleaner Production*, 306, 127264. <https://doi.org/10.1016/j.jclepro.2021.127264>

- Sengphet, K., Sato, T., Fauzi, M. N., & Othman, R. (2013). Porous ceramic bodies using banana stem waste as a pore-forming agent. *Advanced Materials Research*, 858, 131–136. <https://doi.org/10.4028/www.scientific.net/amr.858.131>
- Silva, K. R., Menezes, R. R., Campos, L. F., & Santana, L. N. (2022). A review on the production of porous ceramics using organic and Inorganic Industrial Waste. *Cerâmica*, 68(387), 270–284. <https://doi.org/10.1590/0366-69132022683873309>
- Speight, J. G. (2017). Inorganic Chemistry. *Elsevier eBooks*, 51–110. <https://doi.org/10.1016/b978-0-12-849891-0.00002-3>
- Tantawy, M. A., & Mohamed, R. S. (2017). Middle Eocene clay from Goset Abu Khashier: Geological assessment and utilization with drinking water treatment sludge in brick manufacture. *Applied Clay Science*, 138, 114–124. <https://doi.org/10.1016/j.clay.2017.01.005>
- Vogli, E., Zollfrank, C., Sieber, H., Greil, P., & Mukerji, J. (2012). Manufacturing of biomorphic SIC-ceramics by gas phase infiltration of Wood. *Ceramic Transactions Series*, 33–42. <https://doi.org/10.1002/9781118370872.ch3>
- Warr, L. N. (2021). IMA–CNMNC approved mineral symbols. *Mineralogical Magazine*, 1–30. <https://doi.org/10.1180/mgm.2021.43>
- Xia, B., Wang, Z., Gou, L., Zhang, M., & Guo, M. (2022). Porous mullite ceramics with enhanced compressive strength from fly ash-based ceramic microspheres: Facile synthesis, structure, and performance. *Ceramics International*, 48(8), 10472–10479. <https://doi.org/10.1016/j.ceramint.2021.12.256>

Yurkov, A. (2017). Refractories and carbon cathode materials for aluminum reduction cells.

Refractories for Aluminum, 75–227. https://doi.org/10.1007/978-3-319-53589-0_2

Zhang, Feng, Li, Z., Xu, M., Wang, S., Li, N., & Yang, J. (2022). A review of 3D printed porous ceramics. *Journal of the European Ceramic Society*, 42(8), 3351–3373. <https://doi.org/10.1016/j.jeurceramsoc.2022.02.039>

Zhao, D., Feng, J., Huo, Q., Melosh, N., Fredrickson, G. H., Chmelka, B. F., & Stucky, G. D. (1998). Triblock copolymer syntheses of mesoporous silica with periodic 50 to 300 angstrom pores. *Science*, 279(5350), 548–552. <https://doi.org/10.1126/science.279.5350.548>